.

Seismic Testing of a Full-Scale, Two-Story Masonry Building: Test Procedure and Measured Experimental Response

by

G. Magenes, G.M. Calvi, G.R. Kingsley

From the Report:
Experimental and Numerical Investigation on a brick Masonry Building Prototype - Numerical Prediction of the Experiment, Report 3.0 - G.N.D.T.

University of Pavia, Department of Structural Mechanics

January 1995

SEISMIC TESTING OF A FULL-SCALE, TWO-STORY MASONRY BUILDING: TEST PROCEDURE AND MEASURED EXPERIMENTAL RESPONSE

Guido Magenes[1], Gregory R. Kingsley[2] and G. Michele Calvi[3]

ABSTRACT

The seismic testing of a full-scale two-story masonry building at the University of Pavia provided an opportunity to involve several research groups in the numerical prediction of a complex experiment. In this paper, the testing procedure and results of that test are presented for comparison with the predictions reported in the collected papers which follow. The definition of the displacement history and force pattern applied to the specimen are justified. The progress of cracking and the evolution of the overall response in terms of forces and displacements are presented and discussed.

1. INTRODUCTION

Unreinforced masonry (URM) buildings can present a significant life-safety hazard in seismic zones. It is also acknowledged that in many seismically active areas of the world, URM buildings constitute the major part of the existing building stock, and that wholesale replacement, or even strengthening, is not feasible. The need to address this problem in an efficient and economic manner has generated significant interest in the development of rational assessment, analysis, and retrofit methods which are appropriate for these structures. The formidable inventory and inherent diversity of these buildings demands a rational yet simple approach to assessment, well supported and validated by experimental research. At the same time, the cost of full-scale testing requires that experiments be carefully addressed to support the capability of understanding the mechanisms involved in the structural response to seismic excitation and to improve the capability of modelling the response analytically. This paper summarizes some recent results from an ongoing coordinated research effort designed to contribute to this need, including experimental and analytical work at several institutions.

The research program was designed to provide support for the complete building assessment process, including the following key phases:

[1] Researcher, Dipartimento di Meccanica Strutturale, Università degli Studi di Pavia, Via Abbiategrasso 211, 27100 Pavia, Italy

[2] Senior Engineer, Atkinson-Noland and Associates, Inc., 2619 Spruce St., Boulder, 80302 Colorado, USA

[3] Associate Professor, Dipartimento di Meccanica Strutturale, Università degli Studi di Pavia, Via Abbiategrasso 211, 27100 Pavia, Italy

1. Survey and observation
2. Interpretation of nondestructive testing as compared to the results obtained from detailed destructive laboratory testing
3. Analytical modeling of components and of whole building structures as compared to experimental destructive tests
4. Design of strengthening techniques
5. Analytical modeling of strengthened structures as compared to experiments

Towards this end, the program includes not only static, dynamic, and pseudodynamic experimental tests on URM materials, components and structural systems, but also a full complement of nondestructive tests and assessment methods, involving several research institutions. Both qualitative and quantitative assessment techniques are directed towards support of analytical models for quantitative assessment of the nonlinear response of URM buildings subjected to seismic ground motions. Emphasis is placed on the need for reliable structural models, ranging from sophisticated finite element analyses to simplified engineering approaches, which should however allow a clear interpretation of the results in a rational way: analysis must relate directly to an engineer's understanding of the fundamental possible response and failure mechanisms.

In previous reports the research plan and the results from preliminary tests were presented [2,3,6]. The main results from the static experimental test on a full-scale, 2-story URM building prototype tested at the University of Pavia are presented in this paper. These results can be compared with the analytical prediction of the response prepared before the tests by several research groups, presented in the other papers collected in this report. Repair and strengthening of the damaged building are being carried out, and future re-testing on the strengthened building is planned.

2. DESCRIPTION OF THE PROTOTYPE

Materials for the structure were chosen to represent typical old urban construction in Italy. Solid fired-clay bricks were used (mean compressive strength on cubes 16 Mpa). The mortar was a mix of hydraulic lime and sand (1:3 volume), giving a compressive strength ranging from 2 to 3 MPa. The measured mean compression strength of masonry prisms was 6.2 MPa. The shear strength of the joint as evaluated from a regression on triplet tests could be expressed as: $\tau = 0.23 + 0.57\ \sigma$ (Mpa). Complete details on material properties can be found in [3].

A simple representation of the geometry of the prototype building is shown in Figure 1. Loading was in the plane of the walls with openings. The building consisted of four two-wythe solid brick walls with a total wall thickness of 250 mm. The plan dimensions were 6 x 4.4 m, and the height was 6.4 m, with non-symmetric openings. One of the longitudinal walls (wall D or "door wall", parallel to the direction of loading) was disconnected from the adjacent transverse walls (walls A and C), while the other (wall B or "window wall") was connected to the adjacent walls with an interlocking brick pattern around the corner.

The floors consisted of a series of isolated steel beams (I section, depth = 140 mm), designed to simulate a very flexible diaphragm. Both vertical and horizontal loads were applied through the floor beams. Concrete blocks were used to simulate gravity loads, for a

total added vertical load of 248.4 kN at the first floor and 236.8 kN at the second floor, corresponding approximately to a distributed load of 10 kN/m^2 per floor. The state of stress resulting from dead weight and added load resulted in vertical stresses ranging up to 0.4 - 0.5 MPa at the reduced section between to the openings level at the ground floor. Such stresses correspond to those in a structure larger than the test prototype, with floors extending on both sides of a wall or to a higher number of stories. The seismic forces were simulated by the application of four concentrated horizontal forces applied at the two longitudinal walls at the floor levels as shown in Figure 2. The horizontal actions were introduced into the floors at the intersections between floors and beams, by means of four displacement-controlled screw jacks.

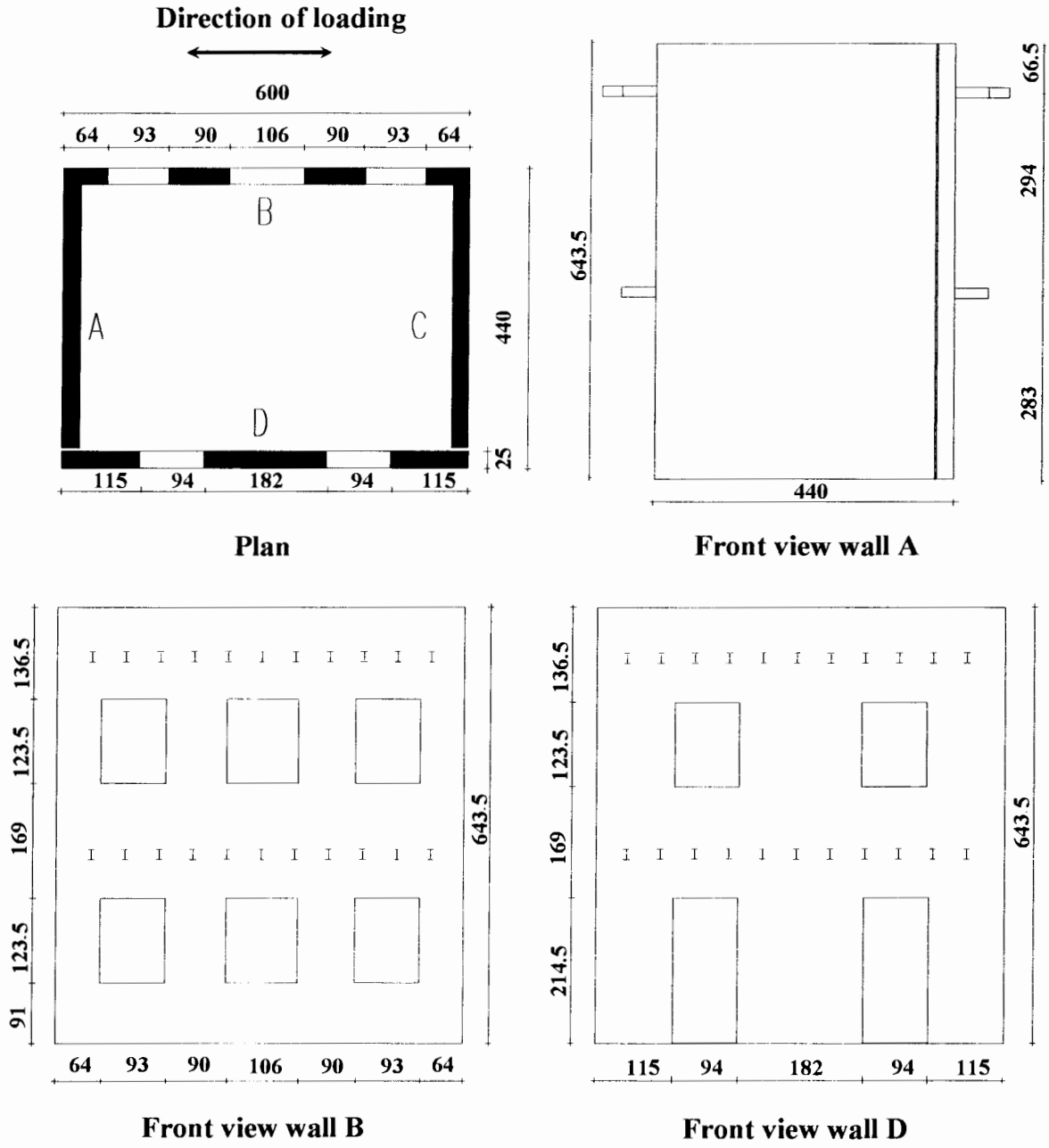

Figure 1. Plan, front, lateral views and dimensions of the prototype, dimensions in centimeters.

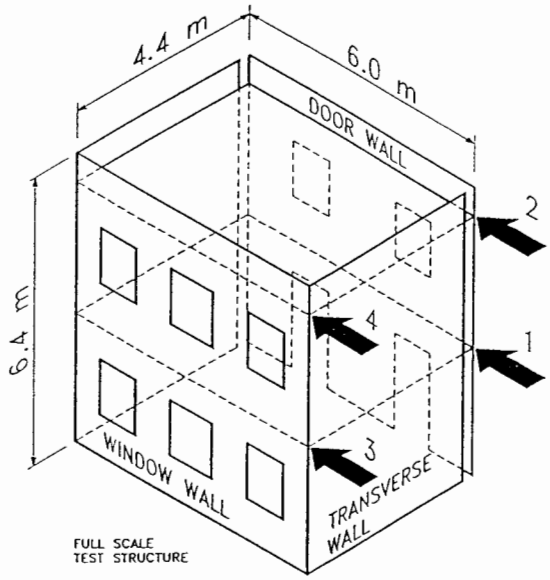

Figure 2. The seismic forces in the full scale static test are simulated with four concentrated forces applied at the longitudinal walls at the floor levels.

3. TESTING PROCEDURE

The prototype building was tested under quasistatic applied displacements programmed to simulate dynamic load/displacement patterns, with reference to a 3/8 scale exact replica of the prototype building tested dynamically on the shaking table at the University of Illinois [1,3]. The motivation of the loading pattern applied to the structure is discussed in the following.

Pseudodynamic testing methods were not considered appropriate for the structure due to difficulties in properly modelling the distributed mass associated with the heavy walls [4]. Furthermore, slow speed simulation of dynamic response was not considered to be realistic for unreinforced masonry (URM) systems in which cracking and damage are highly dependent on loading rate [12]. Instead, dynamic and static methods were effectively combined by deriving the proposed displacement history and loading pattern for the full-scale prototype from the results of shaking table test on a 3/8 scale model of the structure conducted at the University of Illinois.

The shaking table test showed that the behavior of the scaled model was very much dominated by the flexible diaphragms, which supported approximately 60% of the total mass of the building, and had a fundamental frequency less than half of that of the walls [1]. The loads in the walls were therefore associated primarily with the low frequency vibrations of the diaphragms. Because the mass at the two floor levels was the same, and the peak accelerations very similar, the loads at the two floor levels were very nearly equal for much of the test. Similarly, because the floors beams were connected to the walls through pins, the forces in the two walls were equal. The displacements in the walls, on the other hand, were governed by the stiffness of the walls, the development of different damage in the two stories, and a rocking mechanism which developed in the piers of one wall. A constant ratio of displacements was not observed. This is illustrated in Figure 3, showing the ratio of displacements over the duration of one test. The response was highly asymmetrical, with no clear trend in the ratios.

For comparison, Figure 4 shows the effective height of the restoring force for the same test, giving an indication of the force distribution in the walls. An effective height of 0.833 would indicate an inverse triangular distribution, while 0.75 would indicate a uniform distribution. While there is significant scatter in the results, the trend is towards equal forces at both floor levels. It was therefore decided to maintain equal forces at the two floor levels in the quasistatic test; for a two-story structural wall building, the influence of higher modes can be considered negligible, and the choice of a fixed force distribution satisfactory.The problem remained to determine the relationship between the displacements of the two walls: the "door wall" and the "window wall". Figure 5 shows displacement histories from the top of each wall for the three final tests. In the earlier test, the more flexible window wall typically had larger displacements than the door wall, although not in consistent manner, since the relative stiffness of the walls changed with the propagation of cracks. With the development of a rocking mechanism in the door wall in Test 11, the opposite was true for the maximum displacement cycles. Clearly, no constant relationship existed between the displacements of the two walls. However, because coupling through the flexible diaphragms was light in the prototype building, (it was effectively zero in the scale model test), control of this relationship was not critical, and it was decided to maintain equal displacements in the two walls.

Thus the results of the dynamic tests indicated that equal forces should be applied at each floor level in the quasistatic test with equal displacements maintained at the tops of the two walls. It was desired to use the total building drift (the top floor displacement divided by the building height) as the primary controlling parameter of the test, particularly during strength degradation when the stable control of forces alone would not be possible. In order to control both the top displacement and the force distributions in the walls while operating all actuators in displacement control, a control algorithm was developed following the approach used by Igarashi [8]. A brief summary of the algorithm follows.

Consider the four DOF test structure in Figure 2. The problem was to define the vector of target displacements for load increment $(k+1)$ that satisfied the desired force distribution. The constraints on the displacements, $\mathbf{x}^{(k+1)}$, are expressed as

$$\begin{aligned} \{0 \quad 1 \quad 0 \quad 0\}\, \mathrm{x}^{(k+1)} &= \delta_2 \\ \{0 \quad 0 \quad 0 \quad 1\}\, \mathrm{x}^{(k+1)} &= \delta_4 \end{aligned} \tag{1}$$

where δ_2 and δ_4 are the desired target displacements at DOF 2 and 4. The constraints on the forces, $\mathbf{r}$, may be expressed with a series of factors β_i which define the desired relative values of the forces. Note that, because the top displacements are the primary control, the total forces applied are unknown, and only the relative force *distribution* may be specified.

$$\mathrm{r}^{(k+1)} = \begin{Bmatrix} \beta_1 V_1^{(k+1)} \\ \beta_2 V_1^{(k+1)} \\ \beta_3 V_2^{(k+1)} \\ \beta_4 V_2^{(k+1)} \end{Bmatrix} \qquad \begin{matrix} (\beta_1 + \beta_2 = 1) \\ \\ (\beta_3 + \beta_4 = 1) \end{matrix} \tag{2}$$

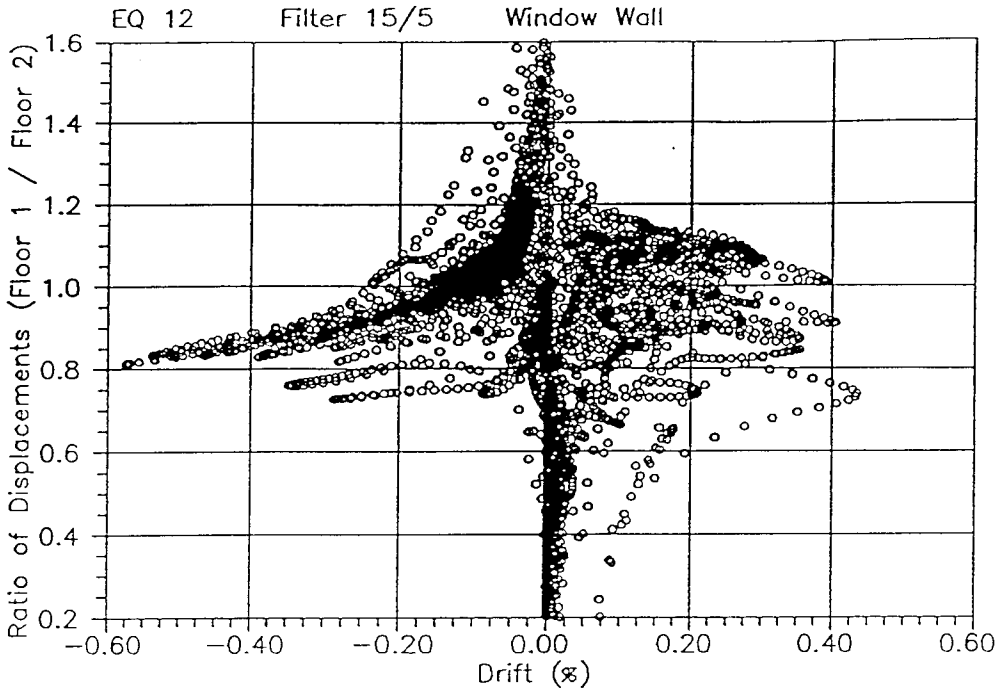

Figure 3. Ratio of first and second floor displacements in the window wall from the dynamic test.

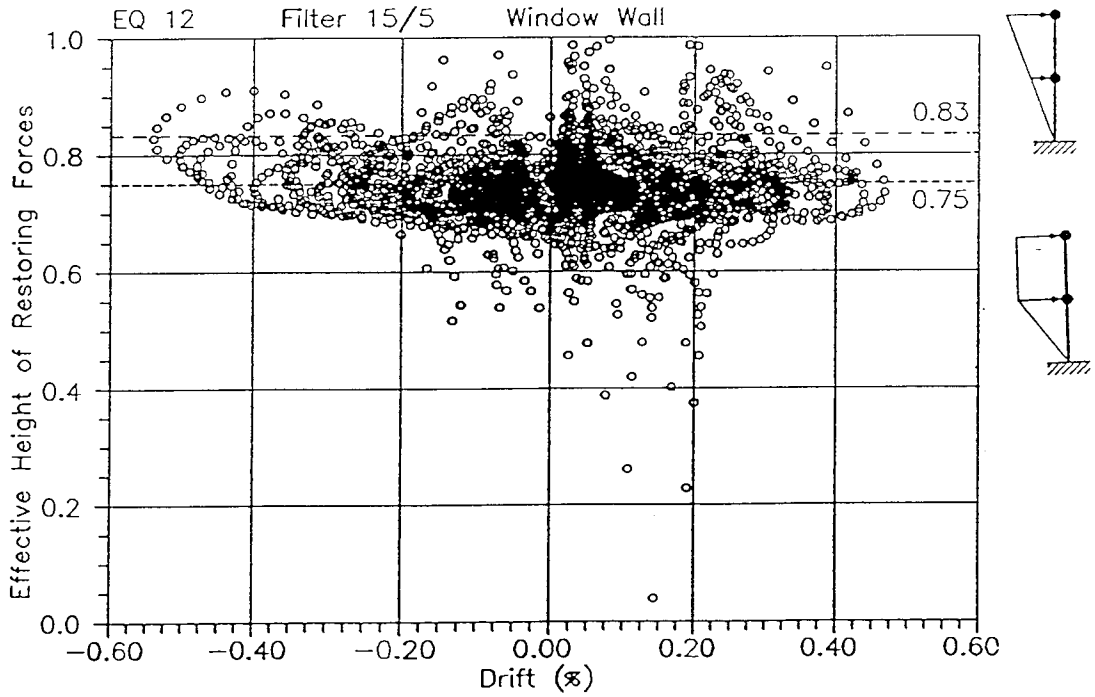

Figure 4. Effective height of the restoring force in the window wall from the dynamic test.

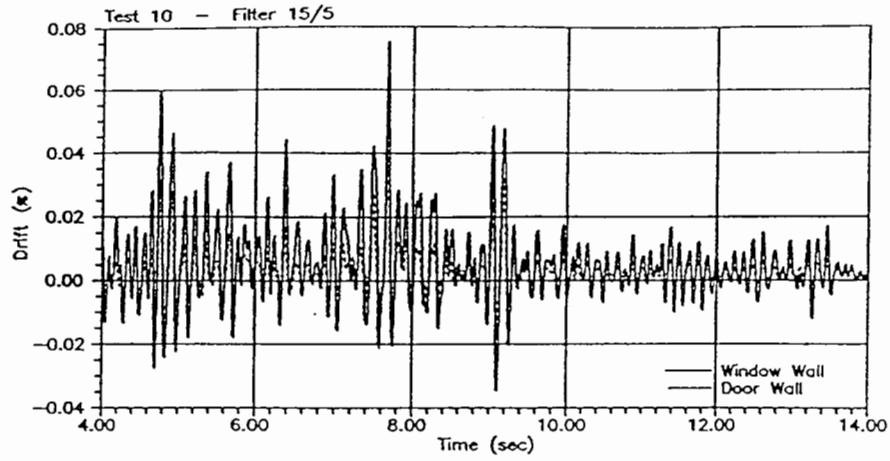

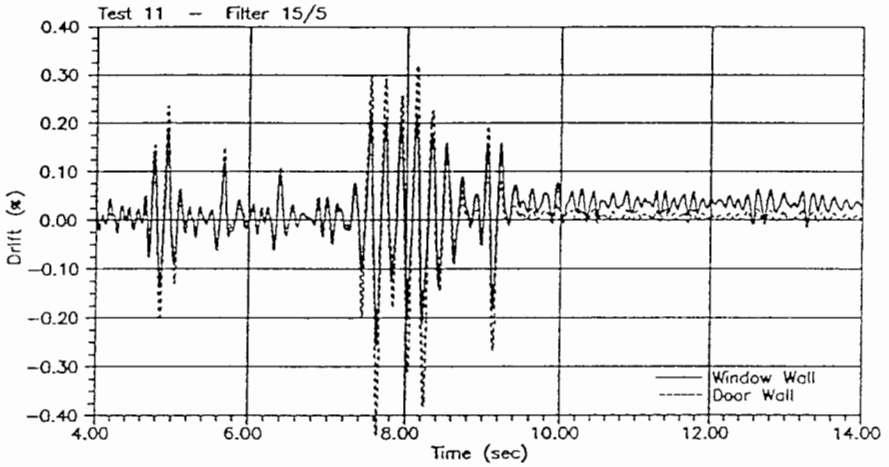

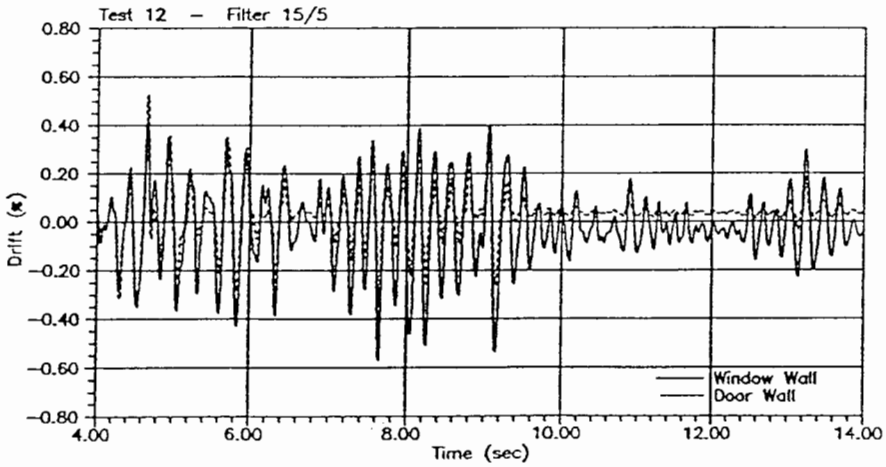

Figure 5. Measured displacement hystories for the two walls from the shaking table tests.

The terms V_1 and V_2 are constants which are equal to the total force applied on each wall at iteration (k+1). For equal forces at the two floor levels of each wall, all factors β_i =0.5

Considering the above constraints, the unknowns are the target displacements at the next step, and the total forces applied in each wall. The unknowns may be found by solving a set of four simultaneous equations of equilibrium with two additional constraint equations [13]:

$$\left[\begin{array}{cccc|cc} & & & & -0.5 & 0 \\ & \hat{\mathbf{K}} & & & -0.5 & 0 \\ & & & & 0 & -0.5 \\ & & & & 0 & -0.5 \\ \hline 0 & 1 & 0 & 0 & 0 & 0 \\ 0 & 0 & 0 & 1 & 0 & 0 \end{array}\right] \left\{\begin{array}{c} \mathbf{x}^{(k+1)} \\ \hline V_1 \\ V_2 \end{array}\right\} = \left\{\begin{array}{c} \hat{\mathbf{K}}\hat{\mathbf{x}}^{(k)} - \hat{\mathbf{r}}^{(k)} \\ \hline \delta_2 \\ \delta_4 \end{array}\right\} \tag{3}$$

where $\hat{\mathbf{K}}$ represents the best current estimate of the structure stiffness matrix. If, due to an inaccurate estimate of the structure stiffness, the applied displacement pattern fails to satisfy the constraint on the loads, the above procedure may be used iteratively at the same target displacement. To improve convergence of the algorithm, the stiffness of the structure was measured at several intervals during the testing. In addition, a "minimal update" procedure [9] was used to update the stiffness matrix estimate in real time during the test.

In terms of the displacement control of the structure, the test was typical of simpler quasistatic tests. However, with the control of the relationship between the forces at the two floor levels as described above, the quasistatic test was successful in capturing the dominant response modes observed in the preliminary dynamic test on the 3/8 scale model, keeping the desired force ratio with a satisfactory degree of approximation.

4. ANALYTICAL PREDICTION OF THE EXPECTED RESPONSE

Before the execution of the destructive test of the building prototype, a test plan was prepared and sent to the research groups who were willing to predict analytically the response. The test plan was described as follows.

Individual Test Runs

The masonry building prototype will be subjected to a sequence of test runs in which the maximum top displacement in each wall will be gradually increased until the maximum desired drift for the run is achieved. Each test will consist of a standard pattern of displacement cycles as represented in Figure 6. Before cracking occurs, the sequence will consist of a single preliminary loading cycle, two cycles at the desired maximum displacement, and one degradation cycle. Following cracking, the number of cycles in each run will be increased to two preliminary loading cycles, three maximum displacement cycles, and two degradation cycles. The preliminary and degradation cycles will have displacements equal to $\alpha\Delta = 0.33\Delta$ *, or one third the maximum run displacement,* Δ*. When tests runs are not executed consecutively, the structure will be left in a zero force condition, and returned to the zero displacement condition before commencing the following test.*

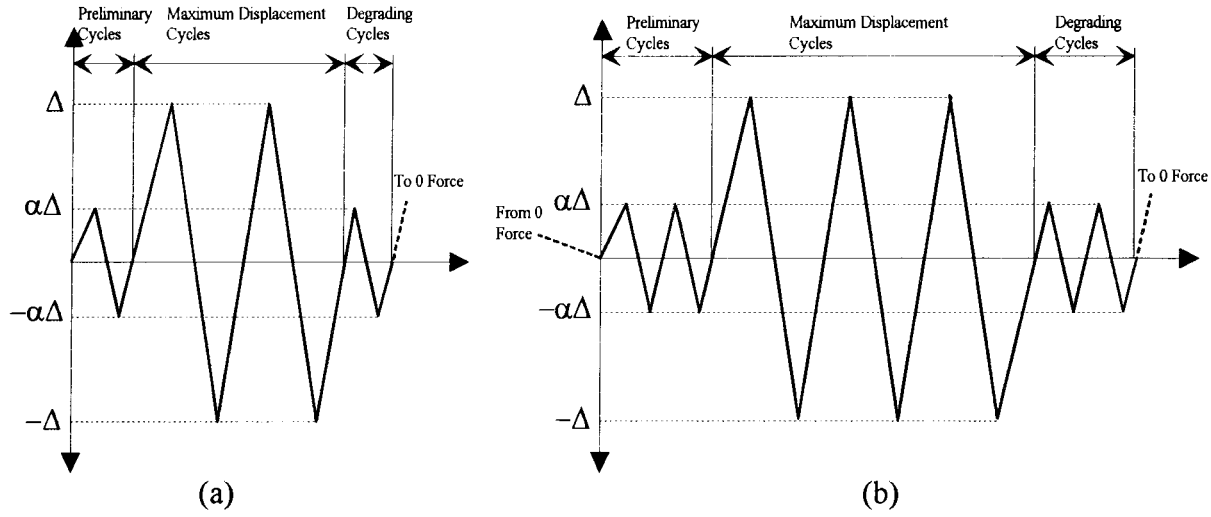

Figure 6. Standardized pattern of displacement cycles (a) Before cracking (b) After cracking

Displacement and Force Distributions

The main controlling parameter for each wall will be the drift, i.e. the top floor displacement divided by the height to the top actuator (5.77 m). The drift of the two walls will be equal for all tests. The displacement at the first floor level of each wall will be controlled such that the applied force at the first floor is equal to the applied force at the top floor level.

Test Sequence

The sequence of target top floor drift and corresponding displacements is listed in the following table.

Run Number	Drift (%)	Displacement (μm)
1	0.025	1442
2	0.050	2885
3	0.075	4328
4	0.100	5770
... until cracking	... + 0.025	... + 1442
5	0.2	11540
6	0.3	17310
7	0.4	23080
8	0.5	28850

It was required to summarize the predicted response following the guidelines given by example forms, as shown in Figure 7, to be prepared for each target drift of the test. Each numerical analyst was therefore requested to report a series of fundamental results, like the drift level at which cracking would have occurred in each wall, and, for each target drift, to indicate the crack distribution, the displacement profiles, the vertical displacements at the corners of the walls, the distribution of the vertical stresses at the base of the walls, the distribution of shears in the wall piers, and the shape of the expected hysteretic curves.

INVESTIGATOR _____ INSTITUTION _____

DATE _____ MAXIMUM DRIFT _____

In the space provided below, sketch (a) the expected damage, (b) the displaced shape, (c) the vertical stress distribution at the wall base, and (d) the shape of the hysteretic curve for the run corresponding to the maximum drift level above. Use the table to indicate the vertical displacements at the top of the wall, and the distribution of shear to the piers.

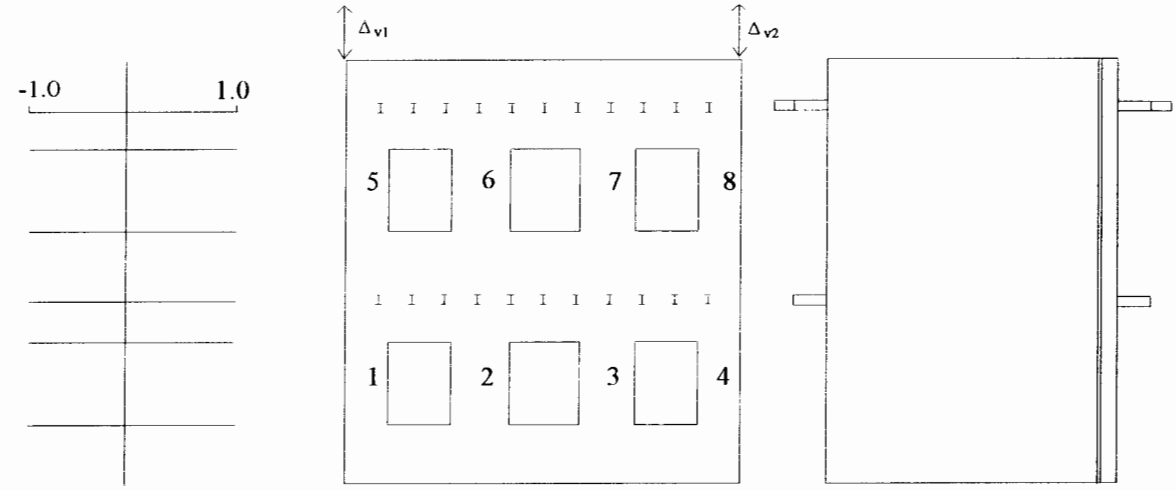

Elevation view wall B

Elevation view wall A

Displaced shape normalized to top floor displacement

Vertical stress distribution at maximum top displacement, normalized to maximum stress.

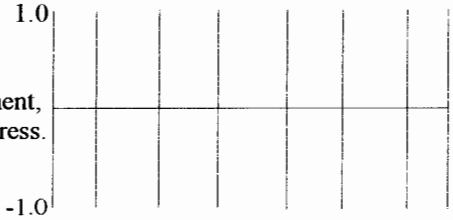

Max. stress=

WALL B

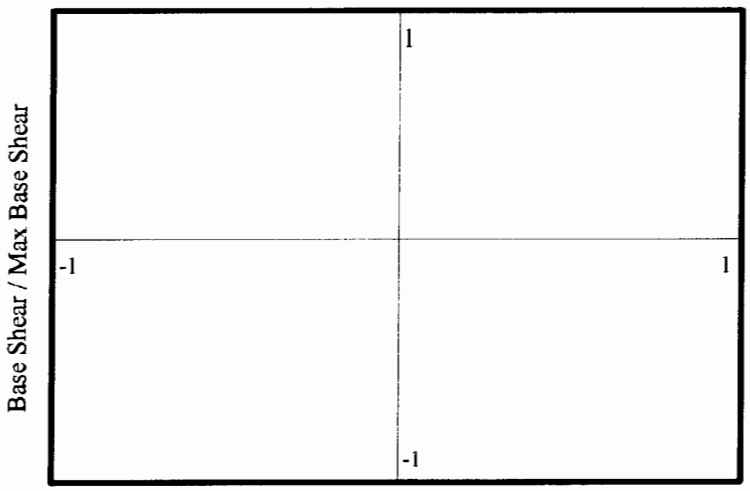

	Positive	Negative
Maximum Base Shear		
Shear in Individual Piers/ Maximum Interstory Shear/ 1		
2		
3		
4		
5		
6		
7		
8		
Δ_{v1}		
Δ_{v2}		

Figure 7. Reference form which was circulated for the collection of the results of the analytical predictions of the test.

All the results already available from preliminary tests on materials were provided to the numerical analysts.

Because of minor modifications decided during the test, the real displacement history imposed to the prototype was not exactly a combination of the standardized patterns given in Figure 6. It is believed that these corrections do not significantly affect the possibility to compare the numerical and the experimental results. The complete experimental displacement history of the top floors is given in Figure 8.

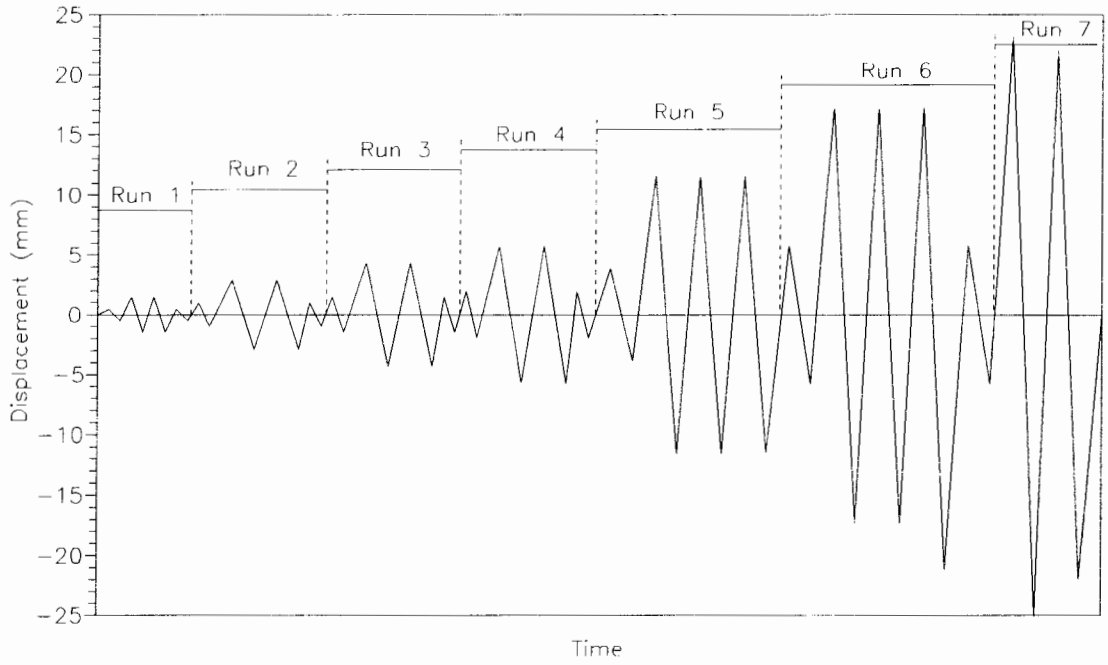

Figure 8. Sequence of displacements applied to the second floor of the prototype.

4. TEST RESULTS

Given the weak coupling given by the flexible floor beams, and the equal displacement applied at the second floor to both longitudinal walls, and since the difference in horizontal displacement between wall B and wall D at the first floor was small when compared to the displacement applied by the jacks, wall D and walls A+B+C constitute in practice two independent structural systems, with negligible longitudinal force transfer through the floors. As a consequence, with reference to Figure 2, the shear applied to the wall D is given by the forces measured in jacks 1 and 2, while the shear applied to walls A+B+C is given by jacks 3 and 4.

The overall response of the structure is summarized in plots of base shear versus top displacement shown in Figures 9 and 10 for the door (D) and window (B) walls respectively. The maximum base shear in the door wall was approximately 150 kN, while the total in the window wall was slightly less at approximately 140 kN. Cracking started at a drift (top displacement / building height) of approximately 0.1%, the maximum horizontal force was initially achieved at a drift of approximately 0.2%. The test was terminated when significant damage had developed in the piers and masonry lintels of the door wall at a maximum drift of approximately 0.4%; only minor degradation of the lateral load carrying capacity had occurred

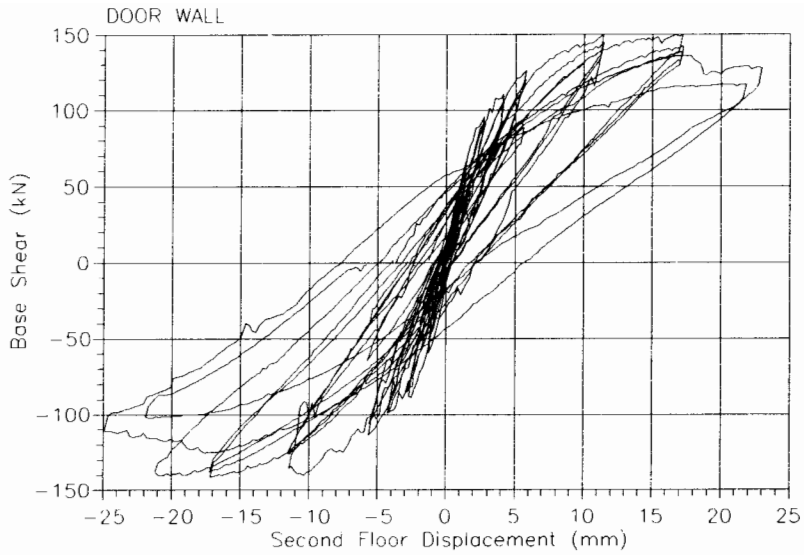

Figure 9. Total base shear vs. second floor displacement, wall D (door wall).

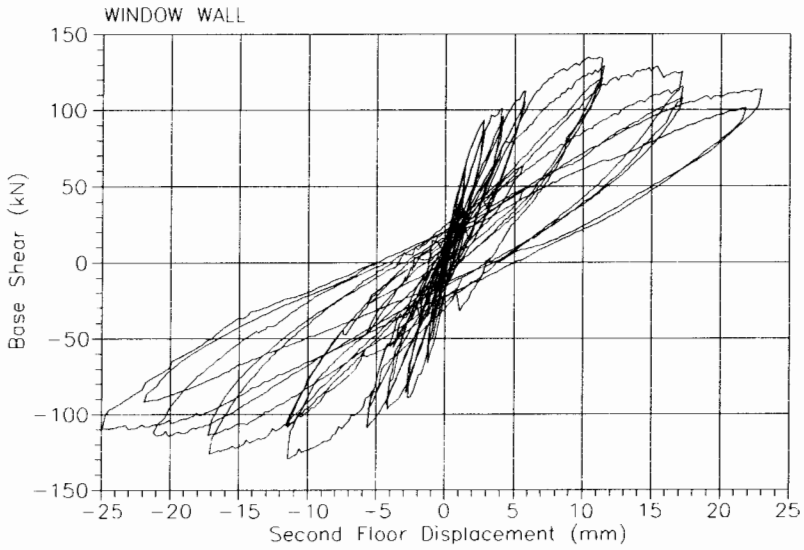

Figure 10. Total base shear vs. second floor displacement, wall B (window wall).

at this point. Since URM structures do not "yield" per se, it is not strictly correct to consider their response in terms of "ductility", however it is worth noting that the test structure achieved an ultimate displacement approximately twice that of the displacement when the maximum load capacity was first attained. The nearly constant load carrying capacity can be attributed to the observed joint-sliding failure mechanism in the critical piers. Even though diagonal cracks developed through both brick and mortar, large local joint sliding displacements were observed during final stages of the test.

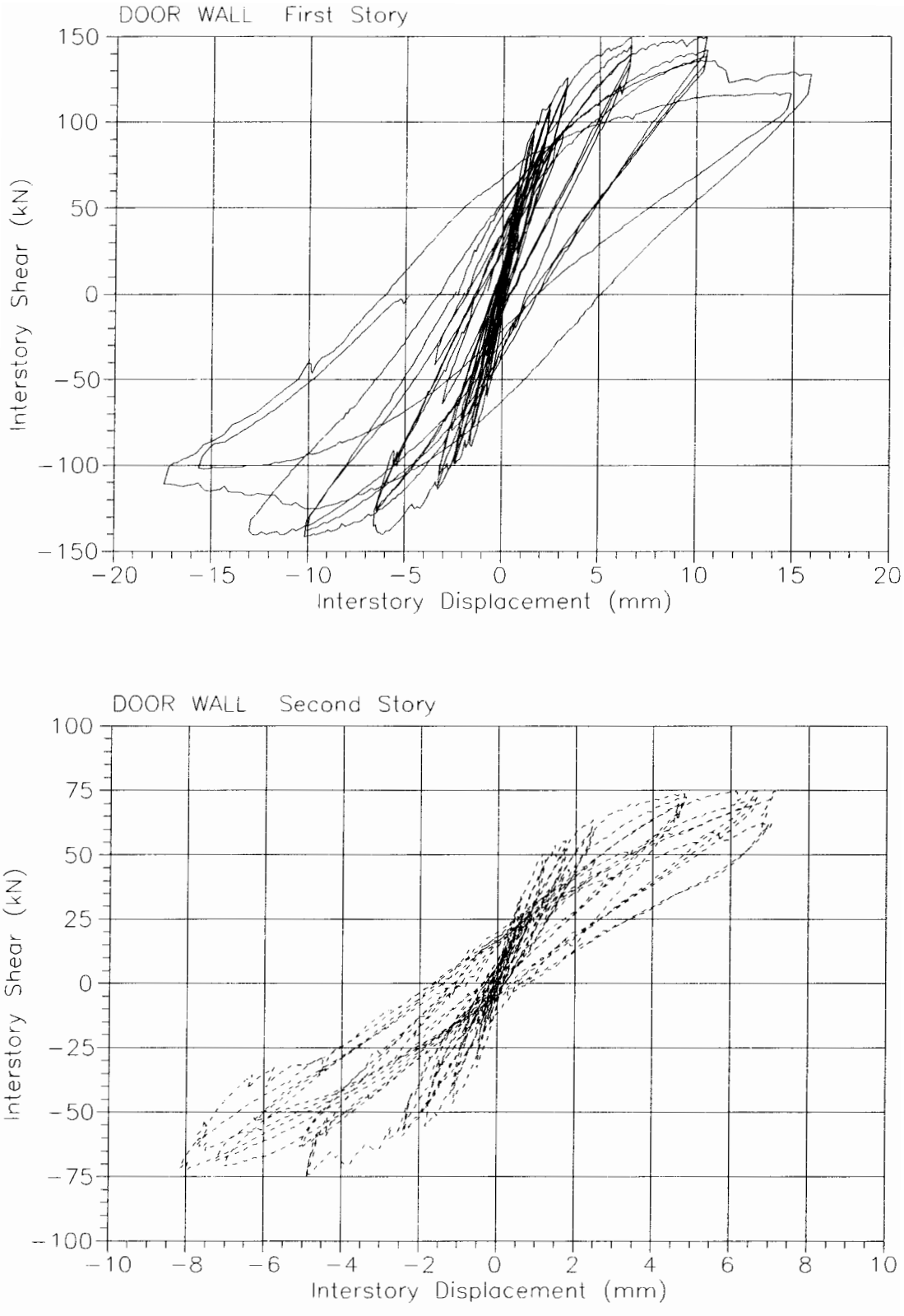

Figure 11. Interstory shear vs. interstory displacement curves, wall D, all runs.

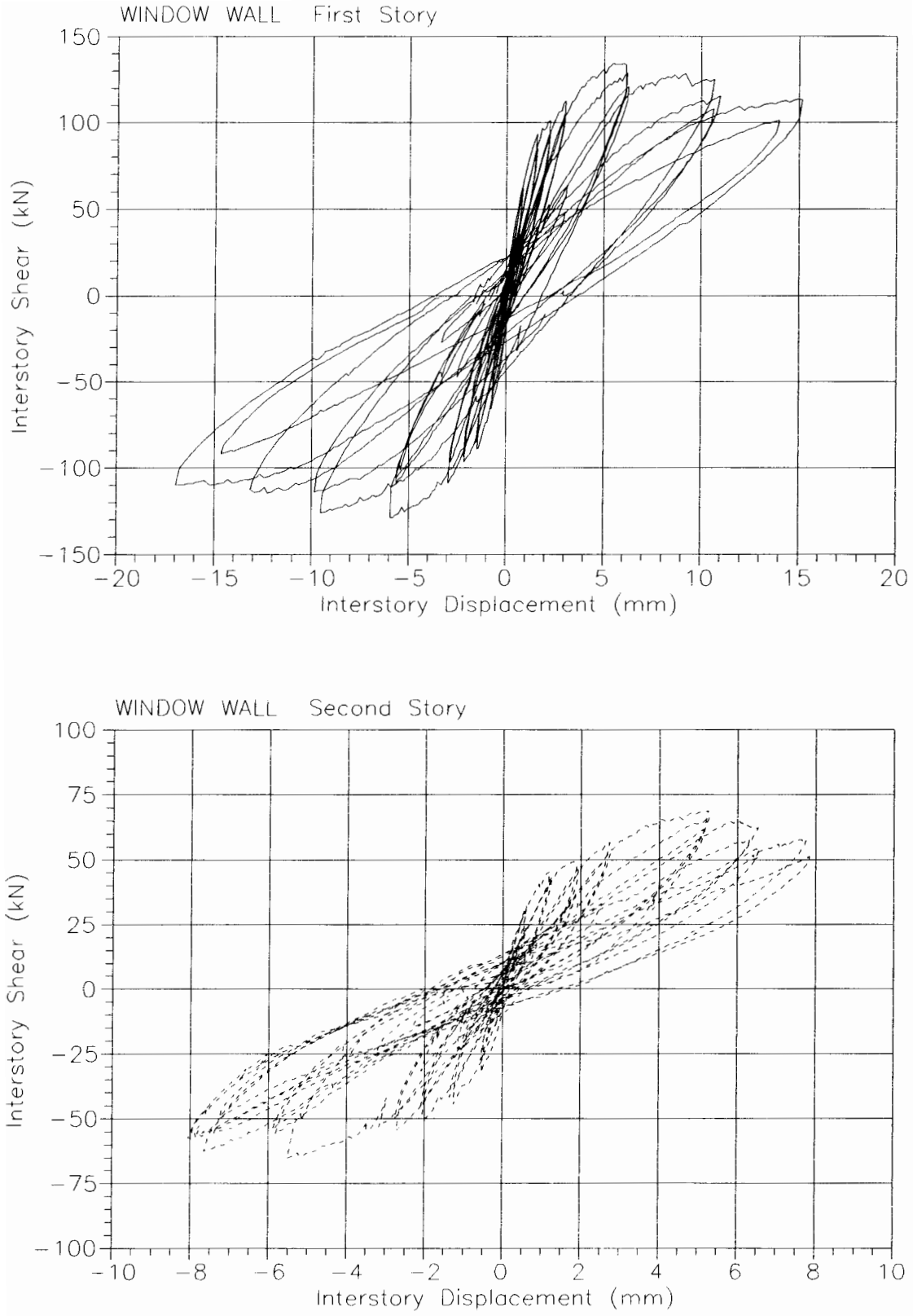

Figure 12. Interstory shear vs. interstory displacement curves, wall W, all runs.

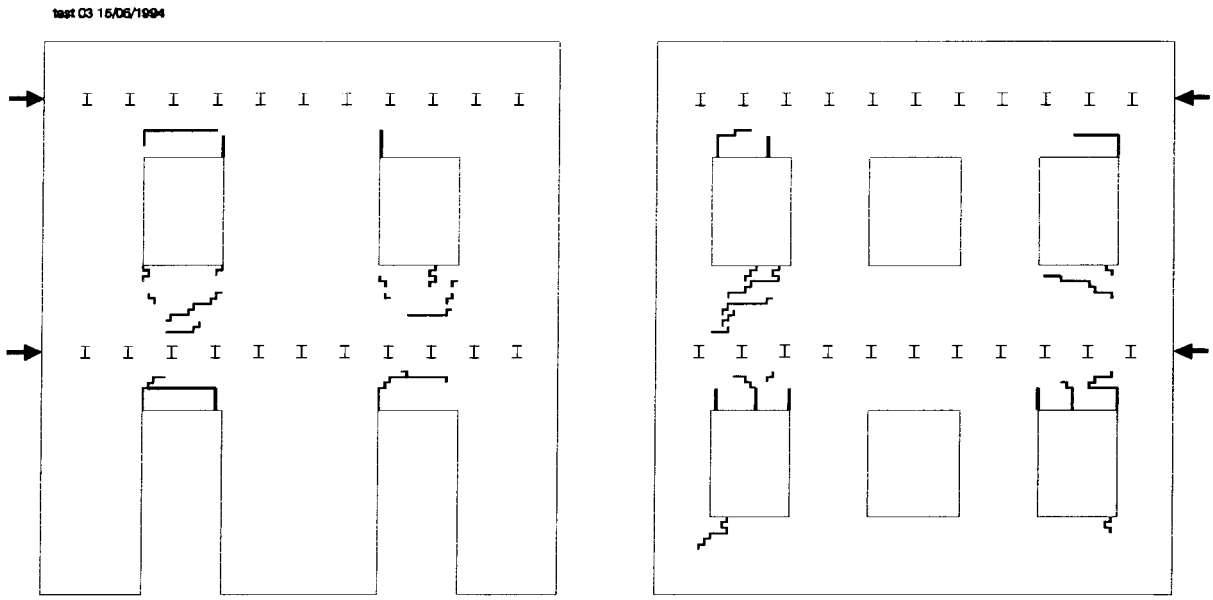

Figure 13. Crack pattern at the end of run 3 (max. drift 0.075%): cracking of spandrels was the first damage occured.

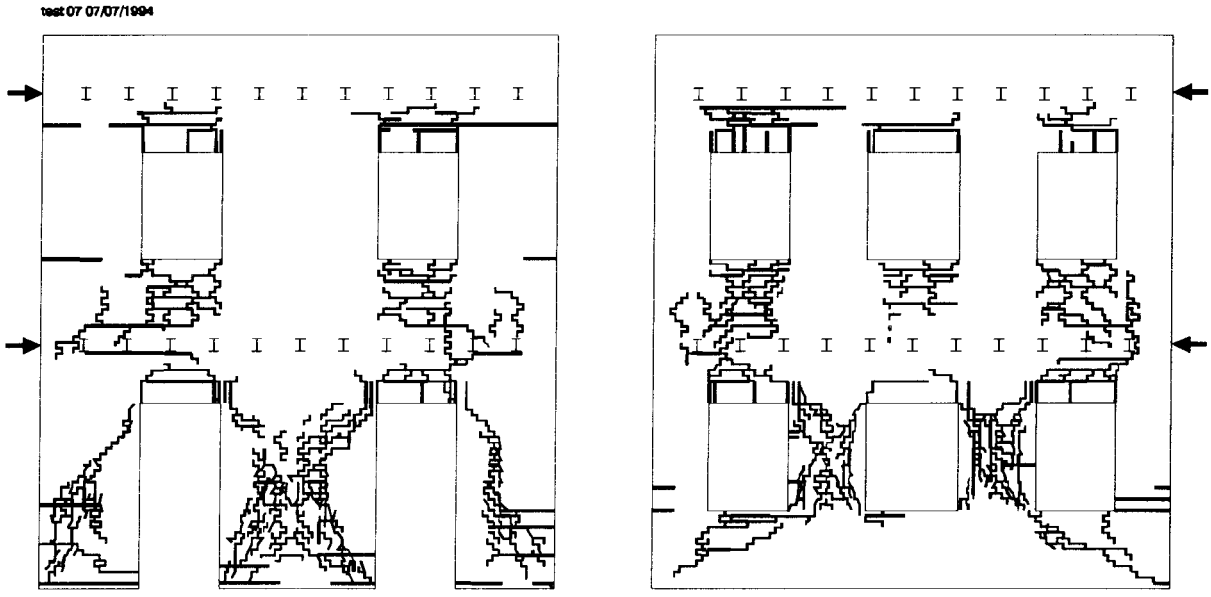

Figure 14. Final crack pattern at the end of run 7 (max. applied drift 0.43 %)

The observed progression of damage in the walls was quite complex, with the nature and location of damage changing significantly with increasing drift. Initially, cracking was limited to the spandrels between the openings in both in-plane walls (see Figures 13 and 14 showing the crack pattern at different drift levels), in part because these regions were not subjected to any vertical stress due to dead loads, and the joint shear strength was therefore less than elsewhere in the structure. As cracks developed in the spandrels, the coupling between the masonry piers decreased; eventually, cracks in the spandrels ceased to propagate further, and the failure mechanism became one dominated by shear cracking in the central piers. At the maximum drift level, exterior piers on the door wall failed in shear, while in the window wall the exterior piers remained essentially undamaged.

The door and window walls responded in a significantly different fashion to the imposed displacements. Measured vertical displacements and an evaluation of the deformation modes of the individual piers indicated that the door wall behaved as a coupled shear wall, with significant vertical displacements due to flexure at the top of the wall. The window wall, on the other hand, exhibited a response characterized by shear deformations localized in the piers, with only small uplift due to flexure. The difference is illustrated in Figures 15 and 16, showing horizontal displacement profiles for the two walls, and in Figure 17 showing representative measured vertical displacements over several cycles of response.

The response of the exterior piers in the two walls was also very different: the exterior piers in window wall exhibited a rocking mode, showing no diagonal cracks throughout the test, while the exterior piers in the door wall eventually failed in shear. The difference in the two walls was due both to the arrangement and aspect ratios of the piers, and to the fact that the window wall was connected to the transverse walls while the door wall was not. It is also important to note that the rocking piers in the window wall did not rock between horizontal cracks defined by the window height, but over a larger distance. It must be also remarked that the exterior piers in the door wall presented diagonal shear cracking only in one direction. This is clearly due to the overturning effect of the horizontal forces, which generated an increase in the axial load in the pier on the side corresponding to the direction of the seismic force, turning the rocking or flexural failure mode to a shear-dominated failure, and a decrease in axial load to the wall on the opposite side.

While the achievement of relatively large drift levels is encouraging, this information should be tempered by the observation in dynamic tests on piers [11] that shear failure can be explosively brittle, and accompanied by a complete loss of integrity. On the other hand, dynamic tests of the 3/8 scale prototype [1] showed rather stable rocking response for a complete building system.

A more complete collection of experimental data is reported in the appendix of this paper.

5. CONCLUSIONS

The aim of this report, more than to present the result of what could be considered as a numerical competition, is to give a panorama of the current state-of-art in structural modelling of masonry buildings, having a clear experimental reference, so that the potential of the different approaches can be appreciated.

As it will be seen in the other papers of this report, the models used by the different research groups for the numerical simulation of the experiment present a rather wide variety of approaches. Most of them are essentially two-dimensional or plane models, in which the third dimension (relevant for walls A+B+C), when considered, is introduced in a simplified manner, defining suitable element thicknesses. The peculiar structural configuration of the prototype

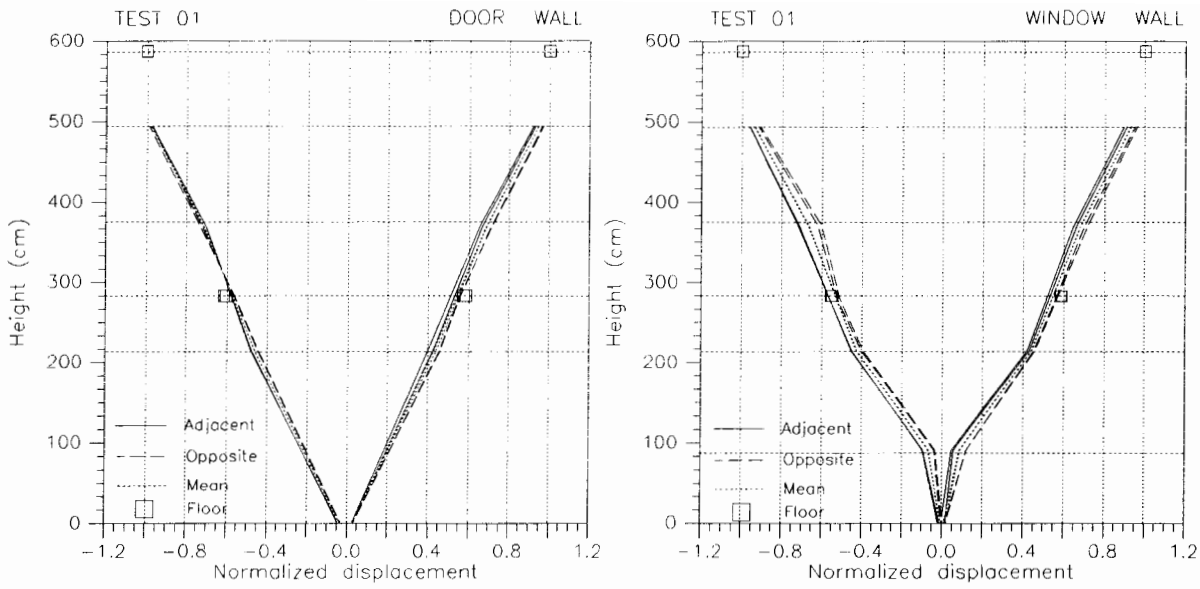

Figure 15. Normalized displacement profiles at thepeaks of run 1
(undamaged state, max.drift= 0.025%)

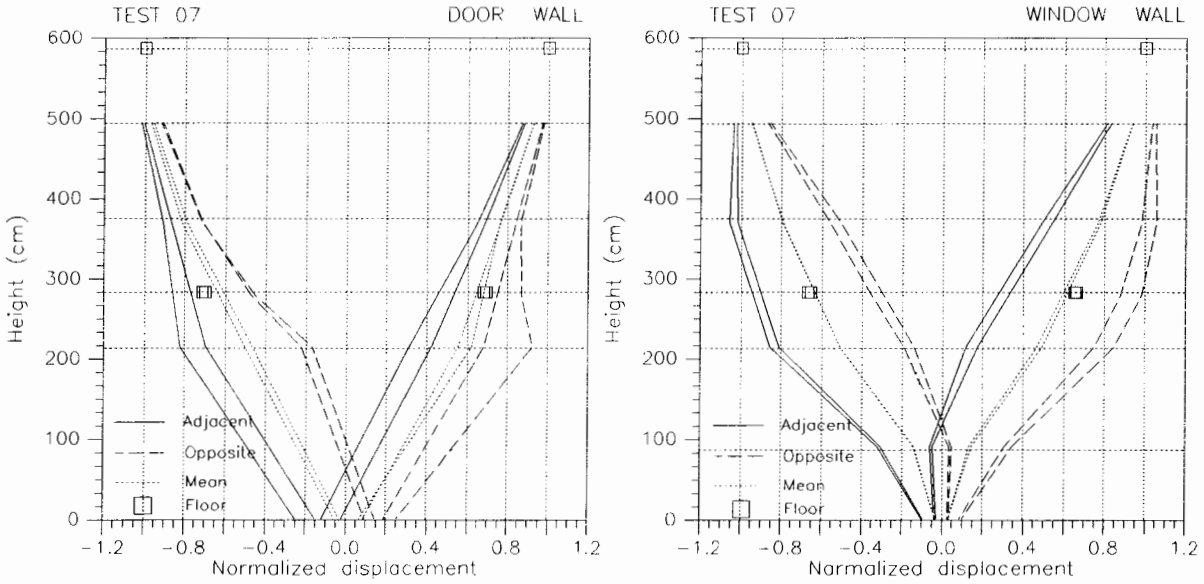

Figure 16. Normalized displacement profiles at the peaks of run 7 (max. drift 0.40-0.43%)

and the testing procedure allow however the idealization of wall D as a plane structure, and to consider wall D and wall A+B+C as independent structures.

Some models are very refined and implement a fully nonlinear cyclic modelling of masonry, while others are only monotonic and aim to the prediction of the envelope of the cyclic response. It will be apparent from the description of the models what is the proper role and applcation for each method, considering the balance between computational effort required, detail and reliability of the results. While the simpler monotonic models can be considered as tools which can be used for assessment in the current practice, the sophisticated nonlinear finite element models, once correctly calibrated, will allow numerical experimentation

with other structural configurations, broadening the spectrum of the research which so far has been limited to the structural configuration and to the materials of the tested prototype.

The experimental data presented in this paper confirm that the failure mechanisms of unreinforced masonry (URM) structures may be quite complex, depending on the interaction of horizontal and vertical components and on the influence of both constant and varying axial loads. Components without axial loads (such as spandrels) are prone to early shear cracking but still the ultimate resistance is given by pier failure. Pier heights other than the clear window height are associated to rocking mechanisms.

The apparently ductile response of the test structure suggests the possibility of a capacity design approach for assessment and strengthening of unreinforced masonry in which a deformation mechanism is selected, and the components selectively strengthened to allow the "ductile" mechanism to occur while inhibiting undesirable shear failure modes. Such an approach is very attractive, but requires additional experimental and numerical verification before being implemented in practice.

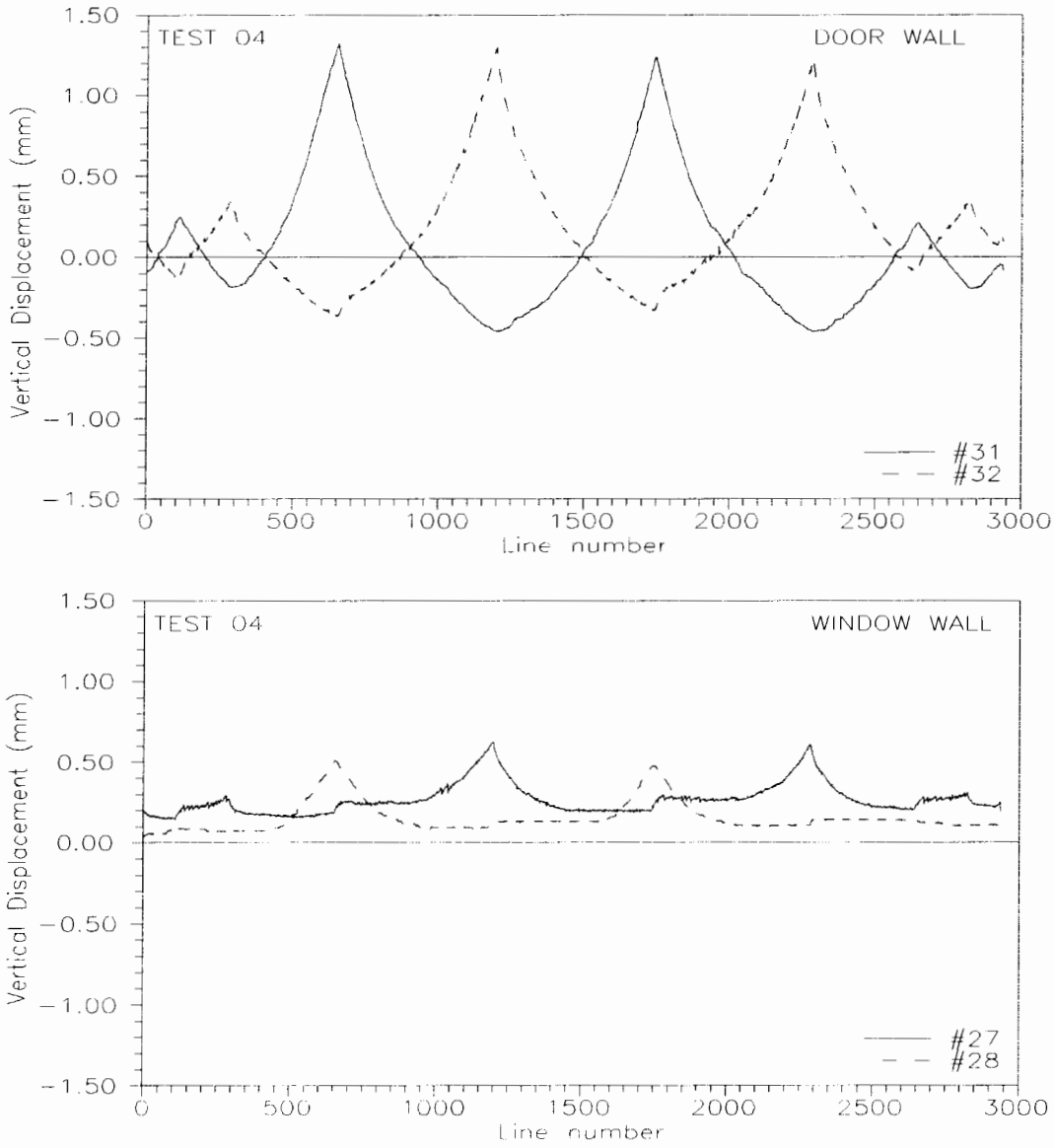

Figure 17. Measured vertical displacements at the top corners of walls D and B, run 4, maximum displacement at the second floor = ±5.77 mm.

REFERENCES

1. Abrams , D.P. and A.C. Costley, Dynamic Response Measurements for URM Building Systems, US-Italian Workshop on Guidelines for Seismic Evaluation and rehabilitation of Unreinforced Masonry Buildings, University of Pavia, Italy, June 22-24, 1994 Report NCEER-94-0021, Buffalo, NY, 1994
2. Ballio, G., G. M. Calvi and G. Magenes (editors), "Experimental and Numerical Investigation on a Brick Masonry Building Prototype - Report 2.0 - Program of scientific co-operations", Dipartimento di Meccanica Strutturale, Università di Pavia, 1993
3. Binda, L., C.Tiraboschi, G.Mirabella Roberti, G.Baronio, and G.Cardani . "Experimental and Numerical Investigation on a Brick Masonry Building Prototype - Report 5.0 - Measuring masonry materials properties: detailed results from an extensive experimental research", Dipartimento di Ingegneria Strutturale, Politecnico di Milano, June 1995
4. Calvi, G.M., and G.R. Kingsley, "Problems and Certainties in the Experimental Simulation of the Seismic Response of MDOF Structures," *Engineering Structures*, (accepted for publication)
5. Calvi, G.M., and M. Nakashima, Sulla sperimentazione pseudodinamica di strutture in muratura, *Ingegneria sismica*, Anno VII - N.3 - September-December 1991.
6. Calvi, G.M., Gi. Magenes, Gu. Magenes, and A. Pavese. "Experimental and Numerical Investigation on a Brick Masonry Building Prototype - Report 1.1 - Design of the Experimental Tests." Dipartimento di Meccanica Strutturale dell'Università di Pavia, February, 1992
7. Costley, A.C., D.P. Abrams, and G.M. Calvi, Shaking-Table Testing of an Unreinforced Brick Masonry Building, Proceedings of the *Fifth U.S. National Conference on Earthquake Engineering*, Vol. 1, Chicago Illinois, July 1994.
8. Igarashi, A., F. Seible, G. Hegemier, M.J.N. Priestley, The U.S. TCCMAR Full-scale Five-story Masonry Research Building Test: Part III - Seismic Load Simulation, *Structural Systems Research Project*, Report SSRP - 94/03, University of California, San Diego, January 1994.
9. Igarashi, A., F.Seible, and G.Hegemier, Development of the Pseudodynamic Technique for Testing a Full-Scale Five-Story Shear Wall Structure, Proceedings of the U.S.-Japan Seminar on the *Development and Future Dimensions of Structural Testing Techniques*, Nikko Waikiki, Hawaii, June 1993.
10. Kingsley, G., F. Seible, M.J.N. Priestley, G. Hegemier, The U.S. TCCMAR Full-scale Five-story Masonry Research Building Test: Part II - Design, Construction, and Test Results, *Structural Systems Research Project*, Report SSRP - 94/02, University of California, San Diego, January 1994.
11. Magenes, G., and G.M.Calvi, "Shaking table tests on brick masonry walls", 10th European Conference on Earthquake Engineering, Vienna, 1994, 2419-2424
12. Paulson, T.J., and D.P. Abrams, Correlation between Static and Dynamic Response of Model Masonry Structures, *Earthquake Spectra,* Journal of EERI, Vol. 6, No. 3, August 1990, 573-592.
13. Seible, F., G.A. Hegemier, A. Igarashi, G.R. Kingsley, Simulated Seismic-Load Tests on Full-Scale Five-Story Masonry Building, *ASCE Journal of Structural Engineering*, Vol. 120, No. 3, March, 1994.

APPENDIX: EXPERIMENTAL DATA FORMS

In the following pages the main experimental data which can be compared with the numerical simulations are collected.

Legend

The following quantities are defined, for each longitudinal wall:

Δ_{h1} horizontal displacement of the first first floor

Δ_{h2} horizontal displacement of the second (top) floor

Δ_{v1} , Δ_{v2} vertical displacements at the upper corners of the wall

F_1 , F_2 resp. applied forces at the first and second floor

F_{tot} total base shear

The values are reported for each major semi-cycle of each run (i.e. the low amplitude cycles of each run are not reported). Note that in some runs the effectively applied displacement and drift at the top floor may differ from the nominal displacement and drift.

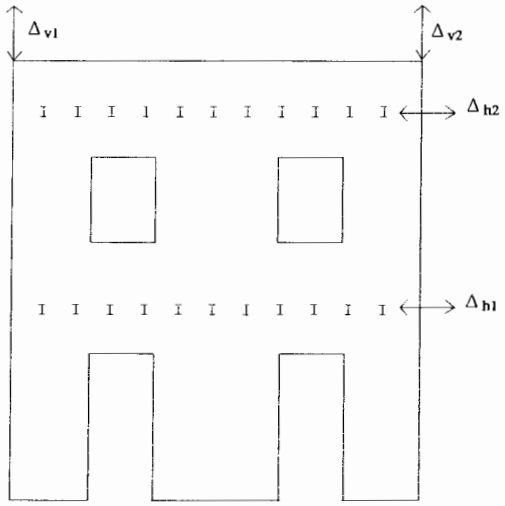

In the normalized displacement profiles, the displacement of the floor beams (symbols □) and three curves are plotted, with the following meaning:

"Adjacent": profile as measured from horizontal displacement transducers applied to the masonry on the wall side adjacent to the jacks;

"Opposite" profile as measured from horizontal displacement transducers applied to the masonry on the wall side opposite to the jacks;

"Mean" curve calculated taking the mean of the "Adjacent" and "Opposite" values.

As the damage (cracking) in the walls proceeds, the displacements measured on opposite sides tend to differ, due to the dilation generated by cracking. The mean curve can be considered as an estimated mean trend of the displaced shape along the height.

UNIVERSITY OF PAVIA - EXPERIMENTAL RESULTS

Date 23/05/1994 - Run 1 - Max. nominal drift: 0.025% - WALL B (Window wall)

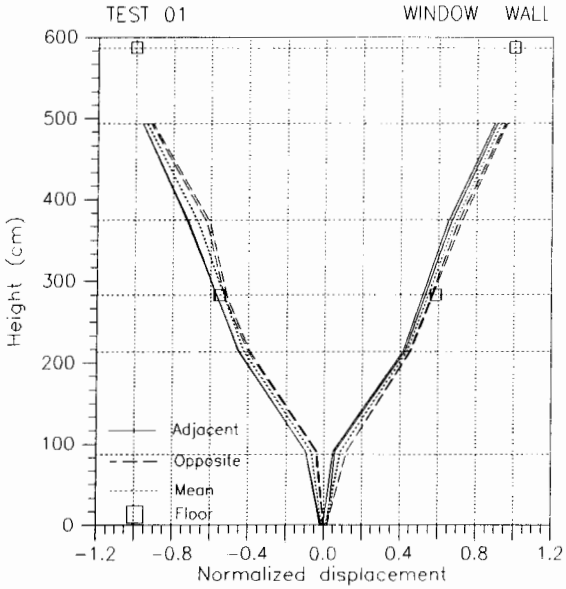

Displaced shape normalized to top floor displacement

Peak	+1'	-1'	+1''	-1''		
Effective drift %	.025	-.022	.025	-.022		
Δ_{h2} (mm)	1.44	-1.30	1.44	-1.26		
Δ_{h1} (mm)	.83	-.75	.84	-.70		
Δ_{v2} (mm)	-.27	.28	-.27	.28		
Δ_{v1} (mm)	.30	-.24	.25	-.23		
F_{tot} (kN)	62.9	-66.0	61.7	-56.3		
F_2 (kN)	32.2	-32.3	30.5	-27.4		
F_1 (kN)	30.7	-33.7	31.2	-28.9		

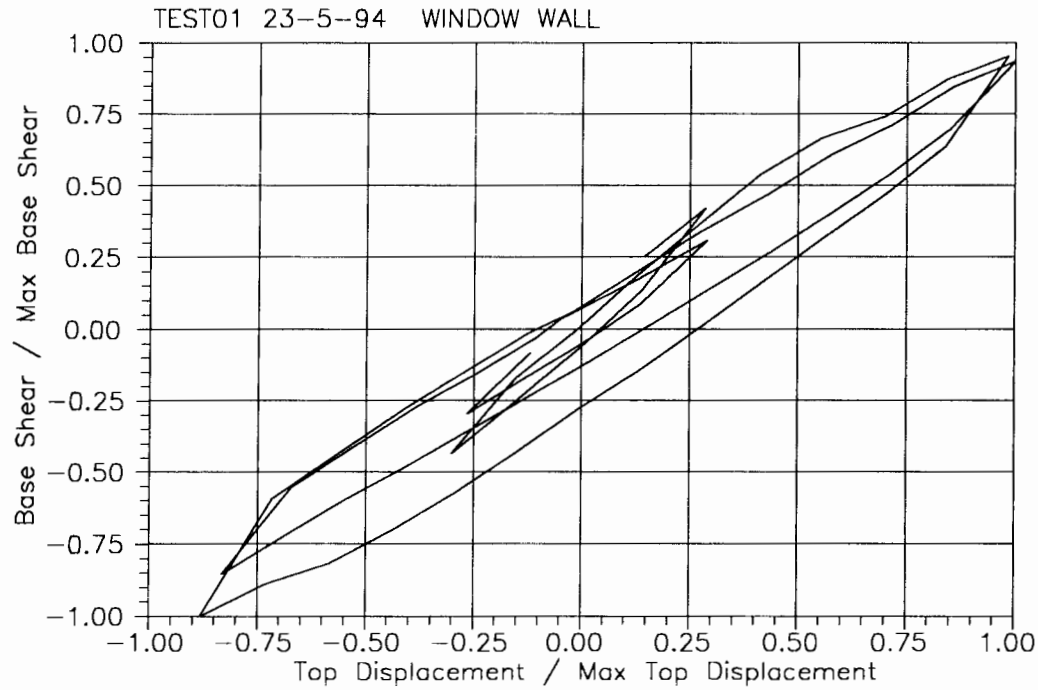

UNIVERSITY OF PAVIA - EXPERIMENTAL RESULTS

Date 23/05/1994 - Run 1 - Max. nominal drift: 0.025% - WALL D (Door wall)

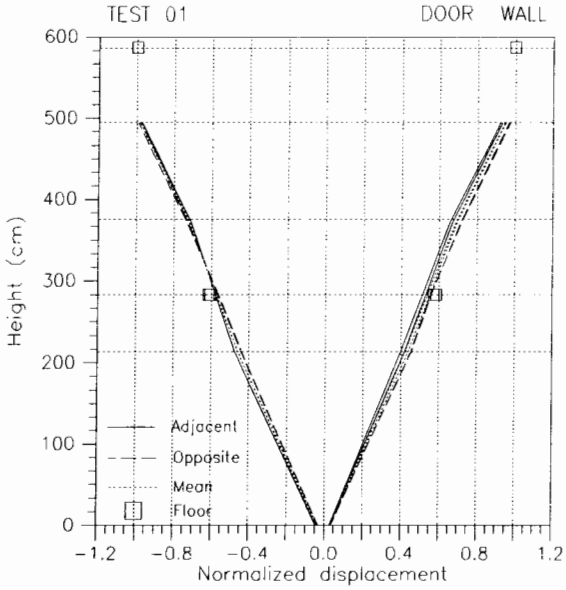

Displaced shape normalized to top floor displacement

Peak	+1'	-1'	+1''	-1''		
Effective drift %	.025	-.022	.025	-.022		
Δ_{h2} (mm)	1.44	-1.29	1.44	-1.27		
Δ_{h1} (mm)	.84	-.76	.83	-.77		
Δ_{v2} (mm)	-.07	.13	-.07	.14		
Δ_{v1} (mm)	.03	-.08	.04	-.06		
F_{tot} (kN)	66.2	-59.5	64.7	-53.7		
F_2 (kN)	33.8	-32.8	32.9	-27.6		
F_1 (kN)	32.4	-26.7	31.8	-26.1		

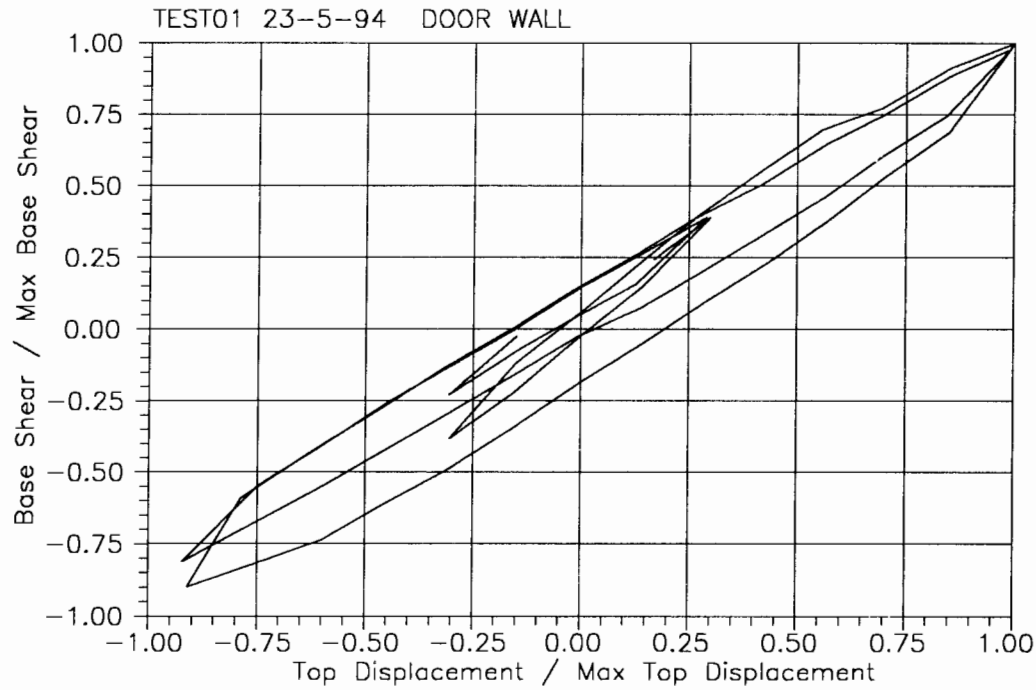

UNIVERSITY OF PAVIA - EXPERIMENTAL RESULTS

Date 23/05/1994 - Run 1 - Max. nominal drift: 0.025%

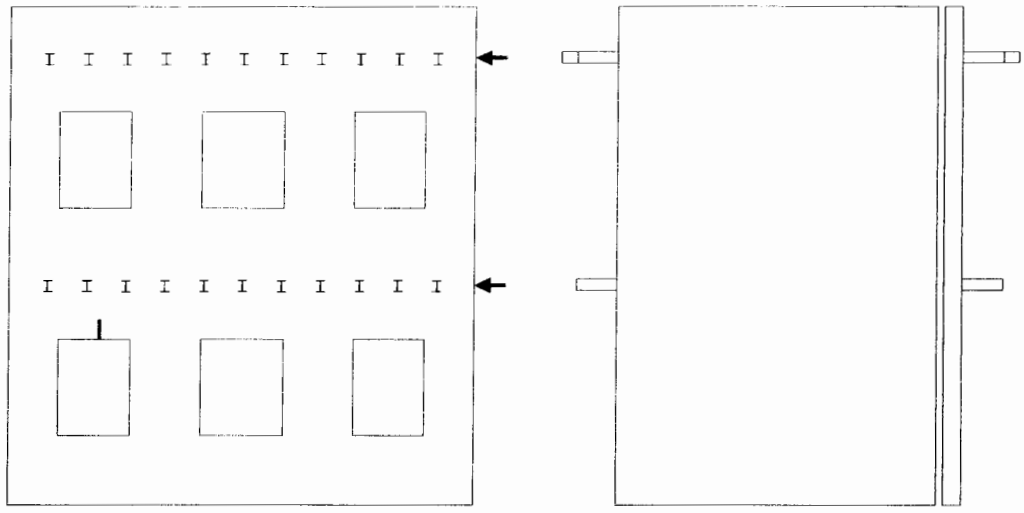

WALL B

WALL A

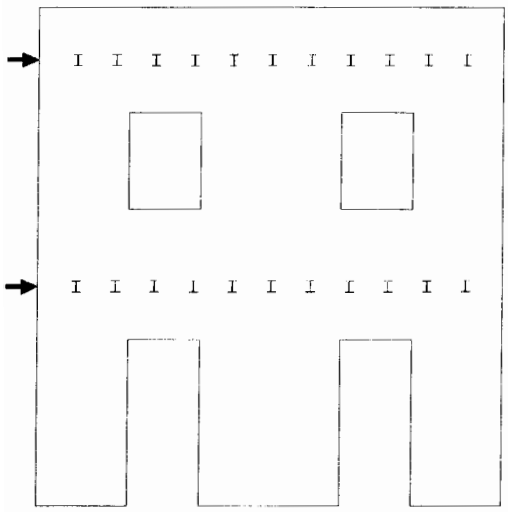

WALL D

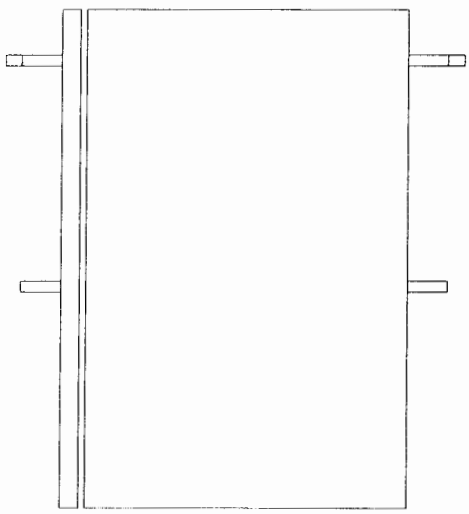

WALL C

Crack patterns at the end of run 1

UNIVERSITY OF PAVIA - EXPERIMENTAL RESULTS

Date 06/06/1994 - Run 2 - Max. nominal drift: 0.050% - WALL B (Window wall)

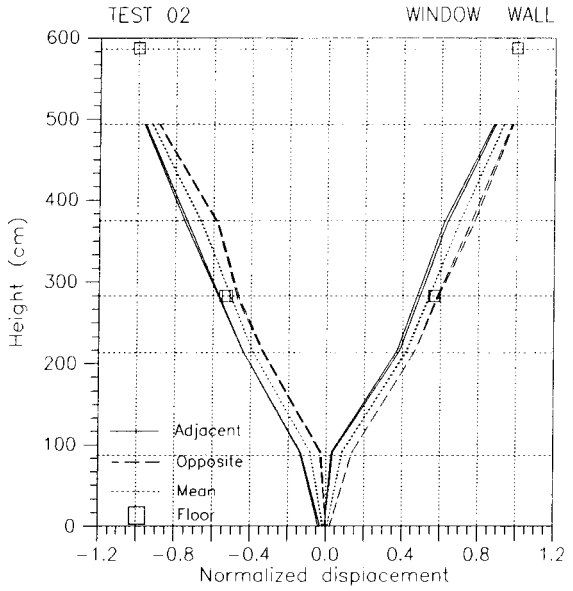

Displaced shape normalized to top floor displacement

Peak	+2'	-2'	+2''	-2''		
Effective drift %	.048	-.048	.049	-.050		
Δ_{h2} (mm)	2.76	-2.75	2.83	-2.88		
Δ_{h1} (mm)	1.57	-1.49	1.57	-1.53		
Δ_{v2} (mm)	-.01	.27	.01	.28		
Δ_{v1} (mm)	.17	-.02	.17	.02		
F_{tot} (kN)	93.4	-89.3	84.8	-85.6		
F_2 (kN)	45.5	-44.5	43.6	-41.7		
F_1 (kN)	47.9	-44.8	41.2	-43.9		

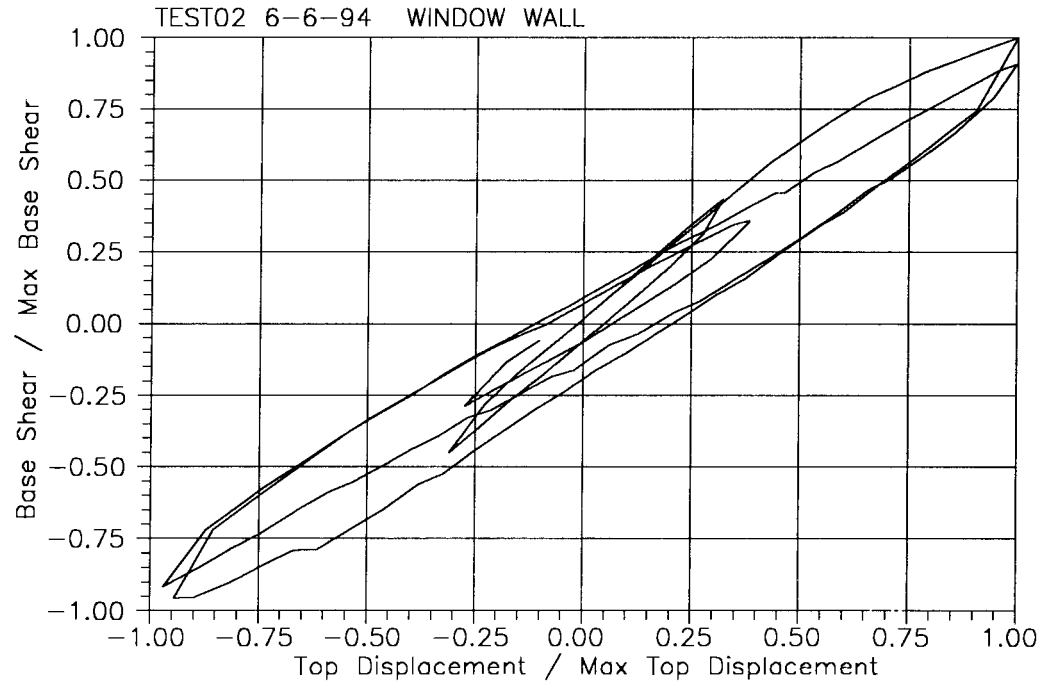

UNIVERSITY OF PAVIA - EXPERIMENTAL RESULTS

Date 06/06/1994 - Run 2 - Max. nominal drift: 0.050% - WALL D (Door wall)

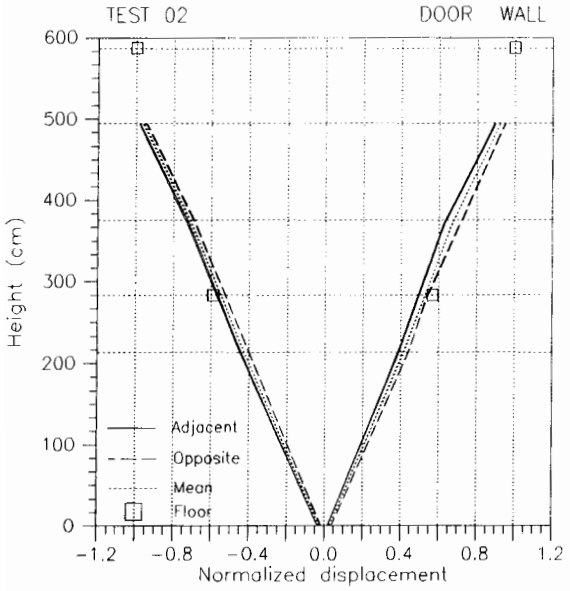

Displaced shape normalized to top floor displacement

Peak	+2'	-2'	+2''	-2''		
Effective drift %	.048	-.048	.049	-.049		
Δ_{h2} (mm)	2.75	-2.74	2.83	-2.85		
Δ_{h1} (mm)	1.58	-1.62	1.59	-1.68		
Δ_{v2} (mm)	-.40	.57	-.36	.57		
Δ_{v1} (mm)	.60	-.34	.56	-.31		
F_{tot} (kN)	95.6	-88.0	91.9	-85.3		
F_2 (kN)	50.4	-46.7	48.1	-41.9		
F_1 (kN)	45.2	-41.3	43.8	43.4		

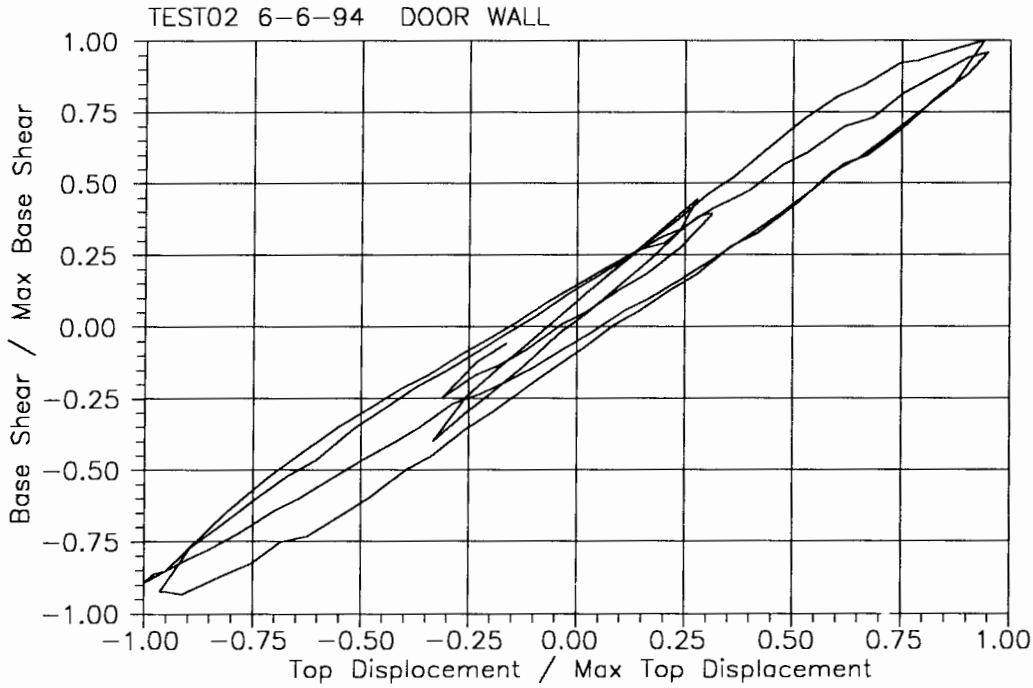

UNIVERSITY OF PAVIA - EXPERIMENTAL RESULTS

Date 06/06/1994 - Run 2 - Max. nominal drift: 0.050%

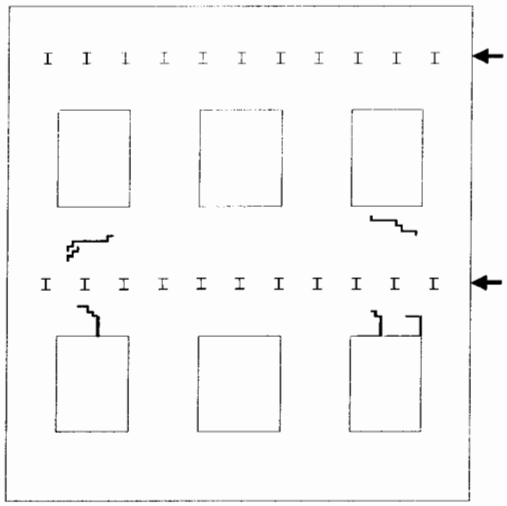

WALL B

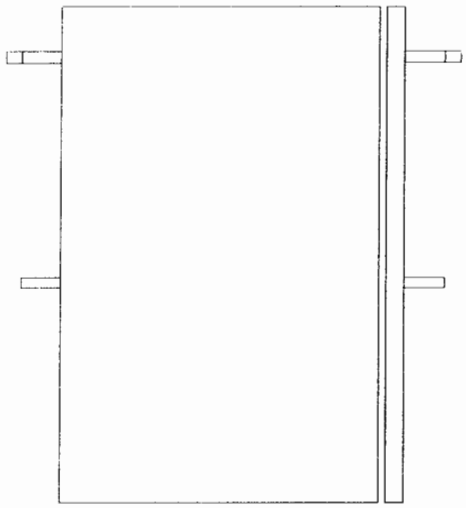

WALL A

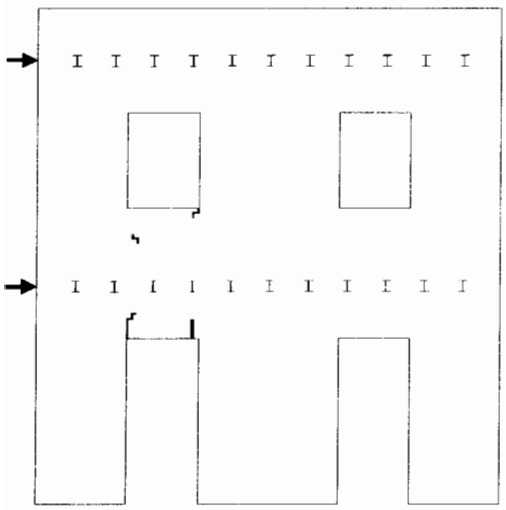

WALL D

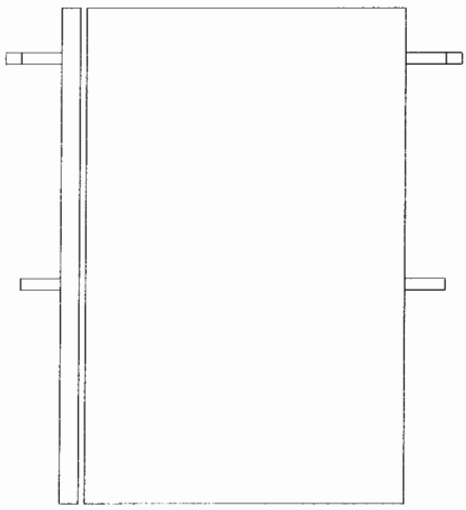

WALL C

Crack patterns at the end of run 2

UNIVERSITY OF PAVIA - EXPERIMENTAL RESULTS

Date 15/06/1994 - Run 3 - Max. nominal drift: 0.075% - WALL B (Window wall)

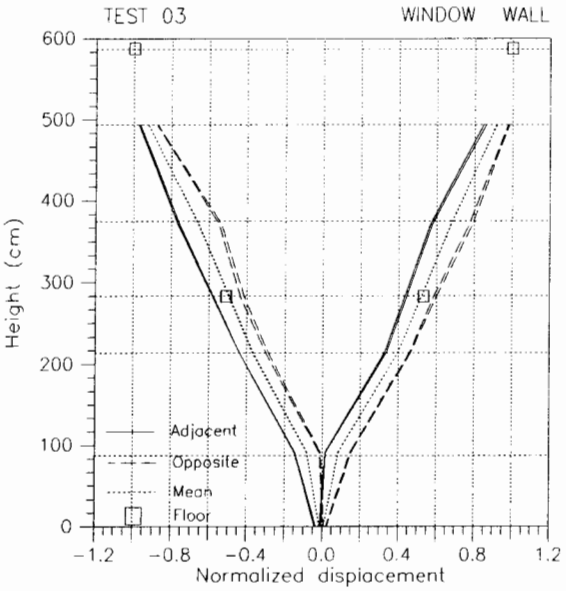

Displaced shape normalized to top floor displacement

Peak	+3'	-3'	+3''	-3''		
Effective drift %	.071	-.073	.072	-.074		
Δ_{h2} (mm)	4.11	-4.22	4.18	-4.27		
Δ_{h1} (mm)	2.22	-2.16	2.24	-2.18		
Δ_{v2} (mm)	.06	.40	.08	.41		
Δ_{v1} (mm)	.28	-.10	.26	.01		
F_{tot} (kN)	101.2	-96.6	95.5	-93.5		
F_2 (kN)	49.4	-48.9	47.4	-45.6		
F_1 (kN)	51.8	-47.7	48.1	-47.9		

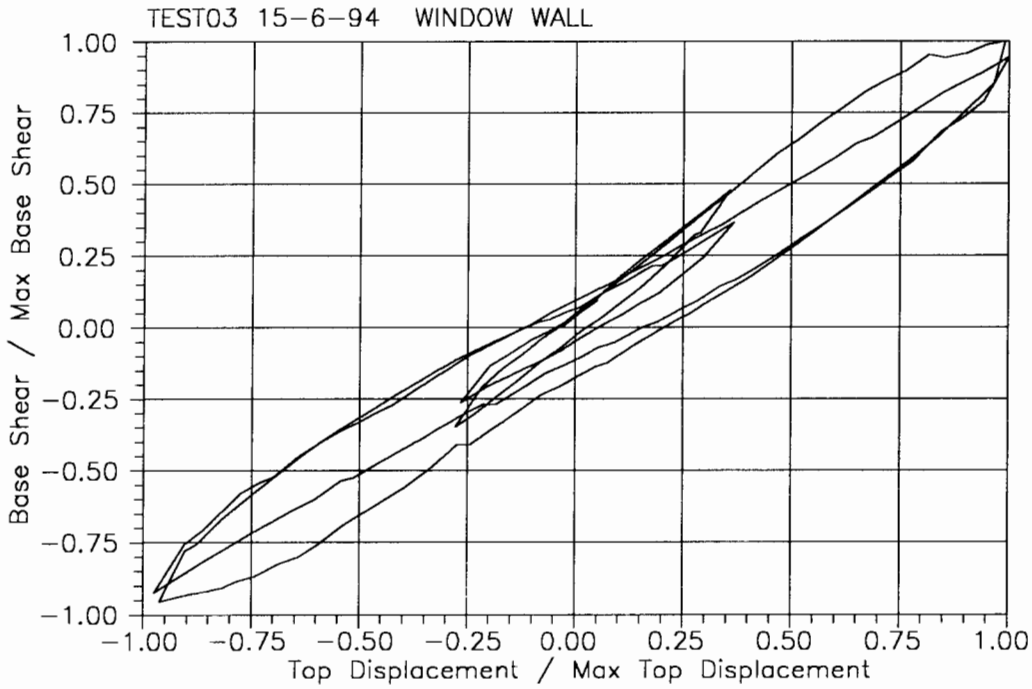

UNIVERSITY OF PAVIA - EXPERIMENTAL RESULTS

Date 15/06/1994 - Run 3 - Max. nominal drift: 0.075% - WALL D (Door wall)

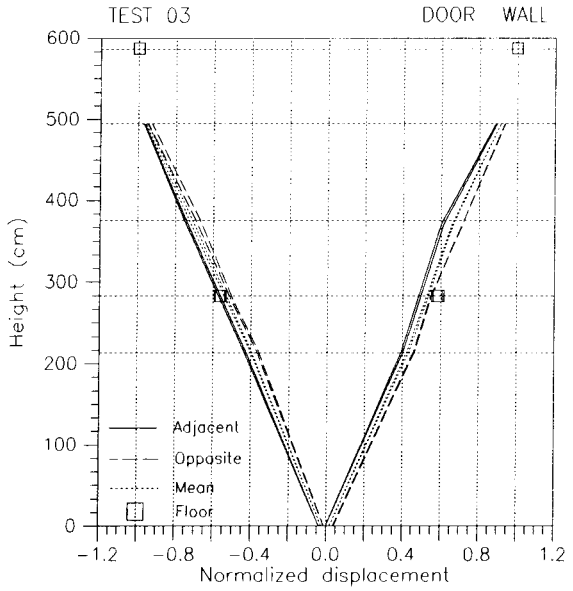

Displaced shape normalized to top floor displacement

Peak	+3'	-3'	+3''	-3''		
Effective drift %	.072	-.073	.072	-.074		
Δ_{h2} (mm)	4.15	-4.22	4.18	-4.27		
Δ_{h1} (mm)	2.41	-2.40	2.40	2.46		
Δ_{v2} (mm)	-.42	.88	-.39	.87		
Δ_{v1} (mm)	.86	-.49	.81	-.47		
F_{tot} (kN)	110.7	-99.1	107.0	-98.9		
F_2 (kN)	55.4	-55.6	52.5	-48.3		
F_1 (kN)	55.3	-43.5	54.5	-50.6		

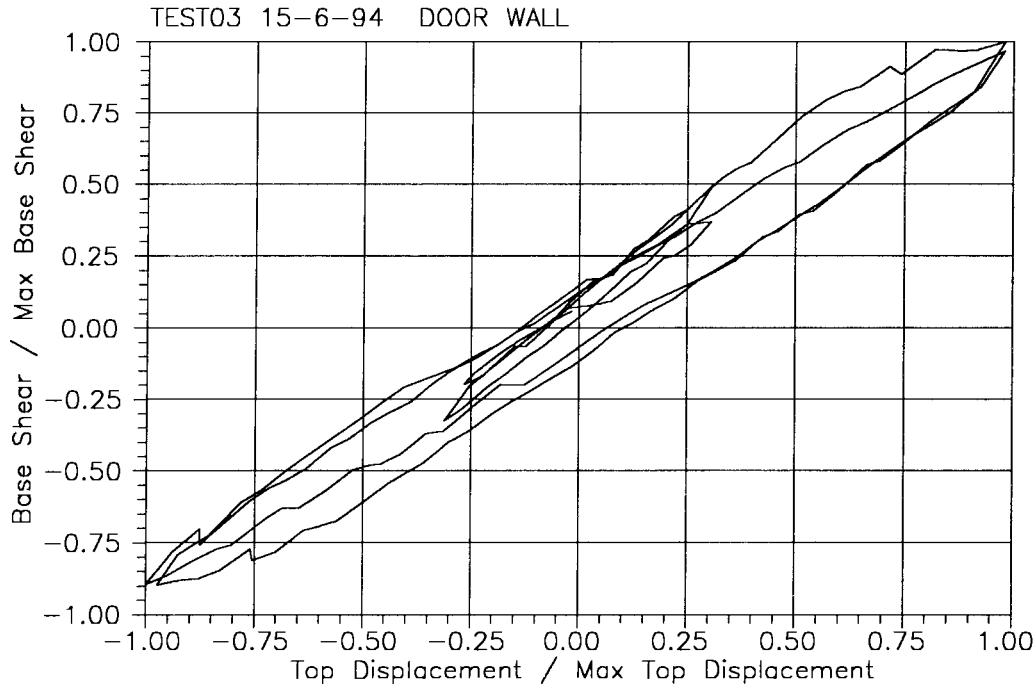

UNIVERSITY OF PAVIA - EXPERIMENTAL RESULTS

Date 15/06/1994 - Run 3 - Max. nominal drift: 0.075%

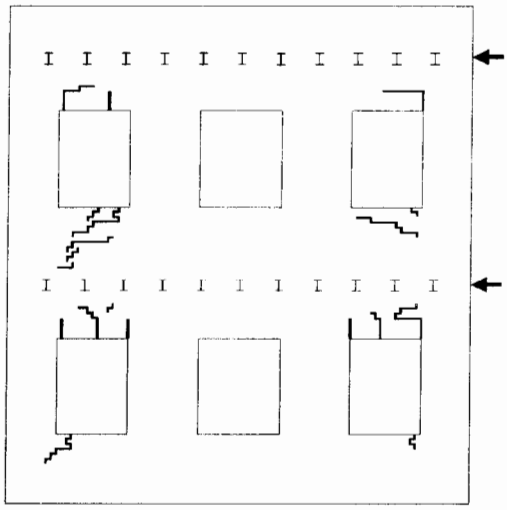

WALL B

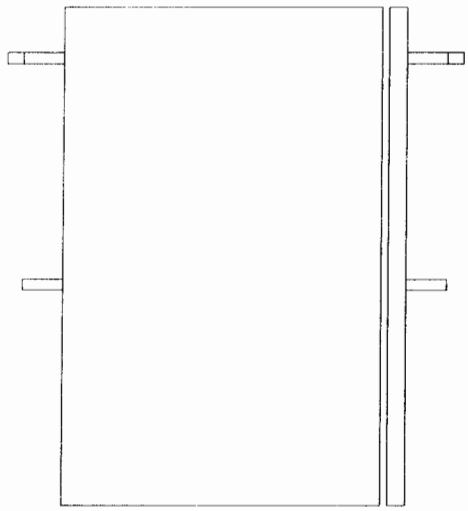

WALL A

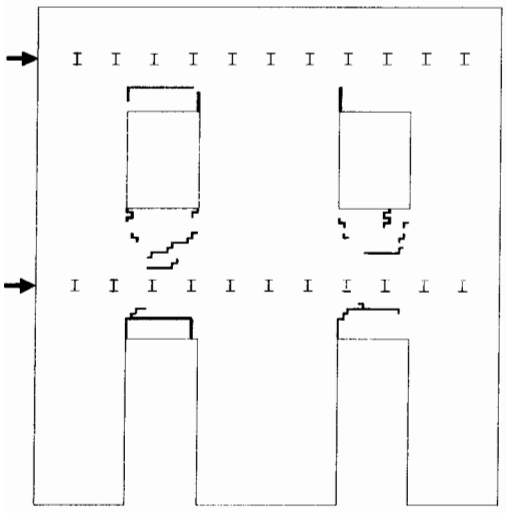

WALL D

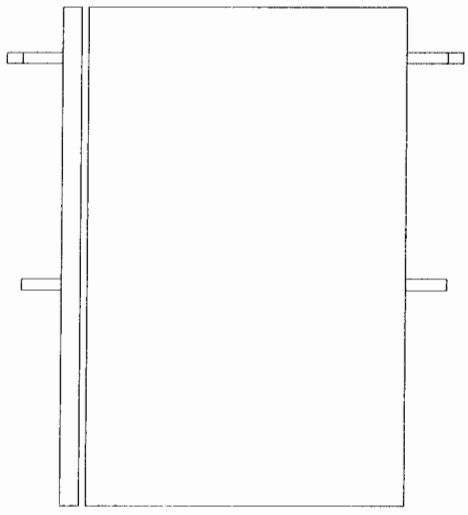

WALL C

Crack patterns at the end of run 3

UNIVERSITY OF PAVIA - EXPERIMENTAL RESULTS

Date 16/06/1994 - Run 4 - Max. nominal drift: 0.10% - WALL B (Window wall)

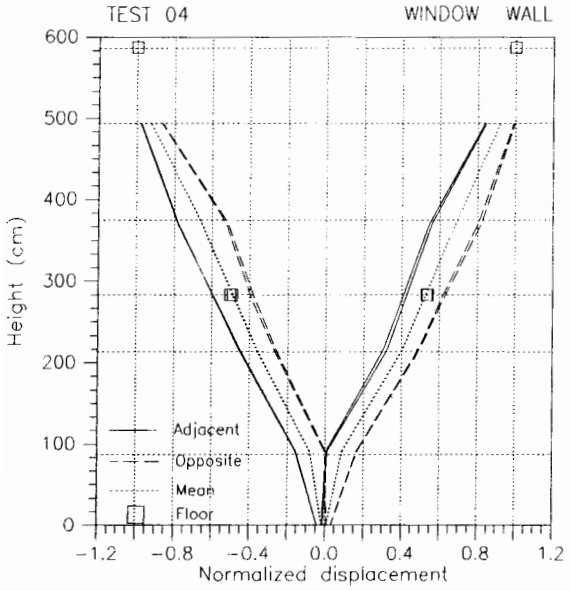

Displaced shape normalized to top floor displacement

Peak	+4'	-4'	+4''	-4''		
Effective drift %	.100	-.098	.099	-..097		
Δ_{h2} (mm)	5.77	-5.66	5.74	-5.59		
Δ_{h1} (mm)	3.04	-2.94	2.99	-2.83		
Δ_{v2} (mm)	.20	.61	.20	.61		
Δ_{v1} (mm)	.51	.11	.47	.11		
F_{tot} (kN)	112.6	-108.7	104.8	-96.8		
F_2 (kN)	56.7	-54.8	52.8	-49.9		
F_1 (kN)	55.9	-53.9	52.0	-46.9		

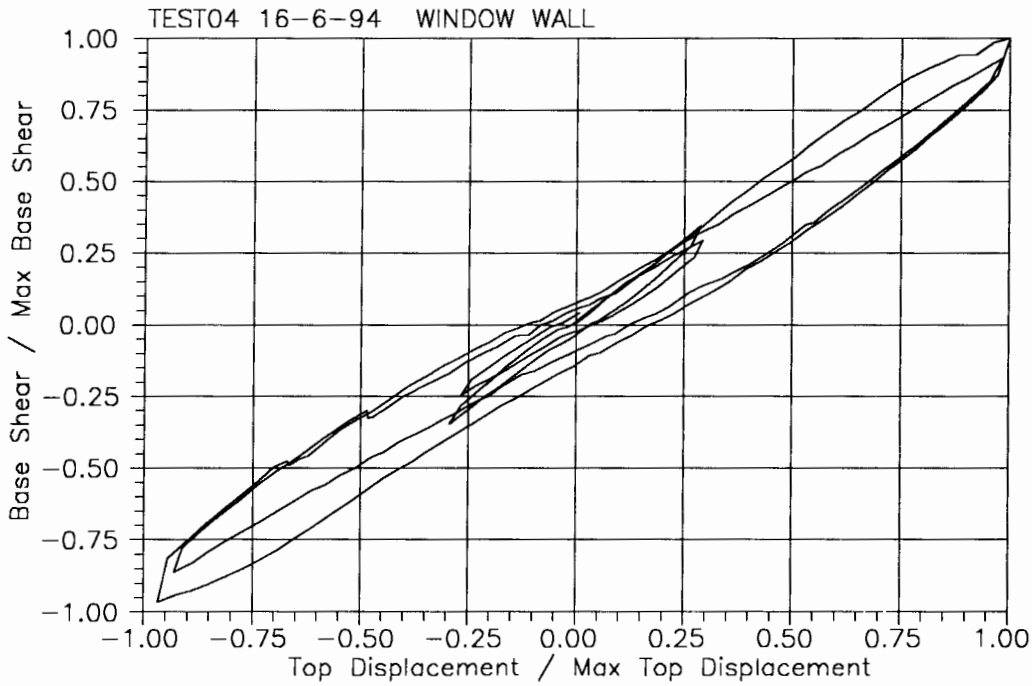

UNIVERSITY OF PAVIA - EXPERIMENTAL RESULTS

Date 16/06/1994 - Run 4 - Max. nominal drift: 0.10% - WALL D (Door wall)

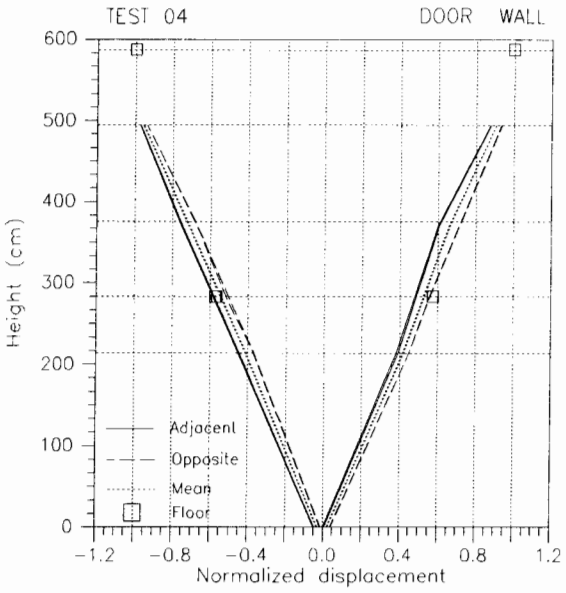

Displaced shape normalized to top floor displacement

Peak	+4'	-4'	+4''	-4''		
Effective drift %	.100	-.098	.099	-.097		
Δ_{h2} (mm)	5.76	-5.65	5.74	-5.60		
Δ_{h1} (mm)	3.30	-3.28	3.26	-3.21		
Δ_{v2} (mm)	-.36	1.26	-.33	1.23		
Δ_{v1} (mm)	1.32	-.46	1.24	-.46		
F_{tot} (kN)	126.1	-113.9	120.3	-106.0		
F_2 (kN)	63.5	-57.0	59.9	-54.8		
F_1 (kN)	62.6	-56.9	60.4	-51.2		

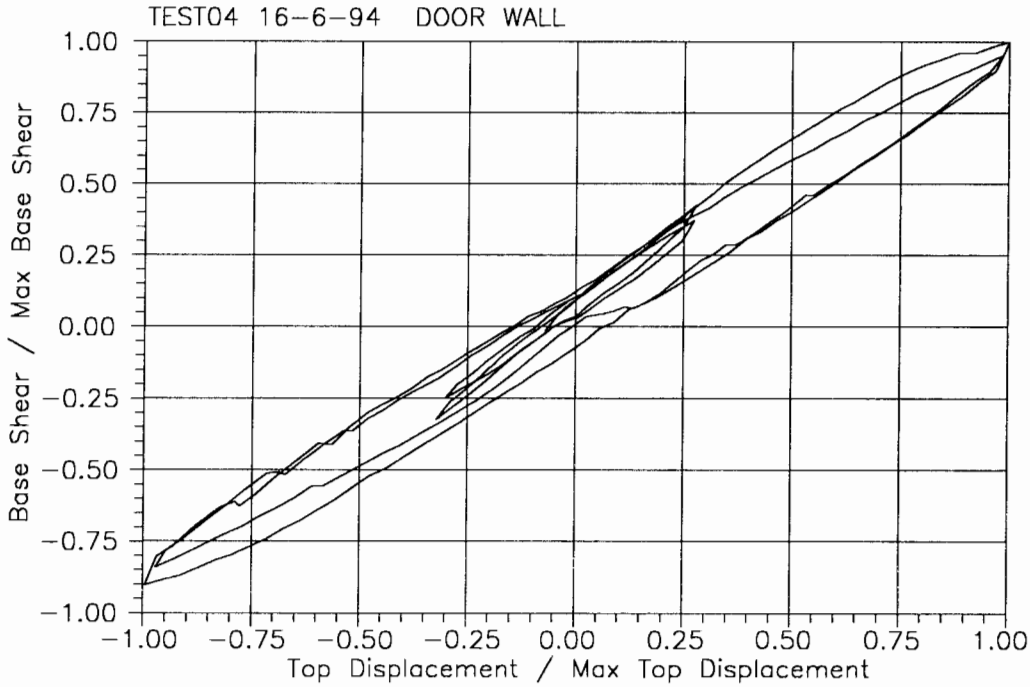

UNIVERSITY OF PAVIA - EXPERIMENTAL RESULTS

Date 16/06/1994 - Run 4 - Max. nominal drift: 0.10%

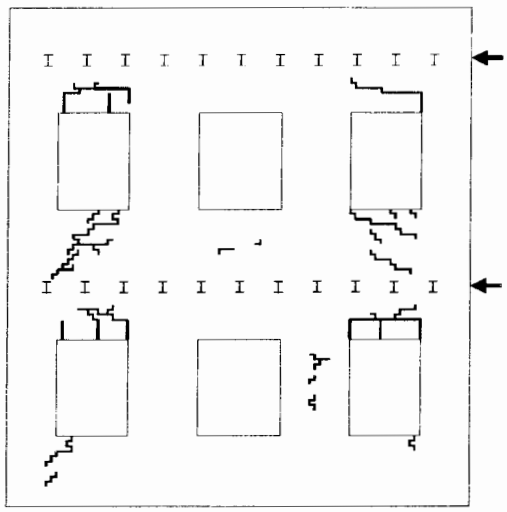

WALL B

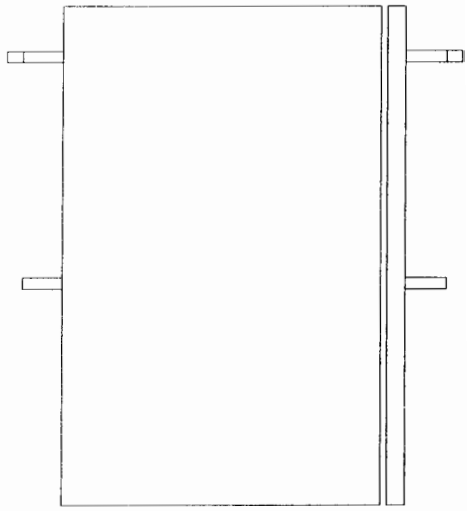

WALL A

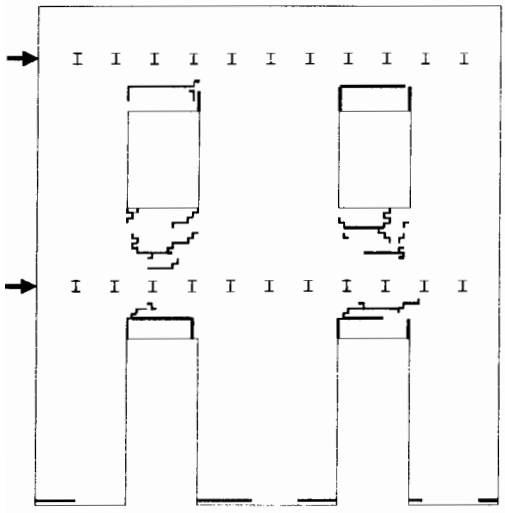

WALL D

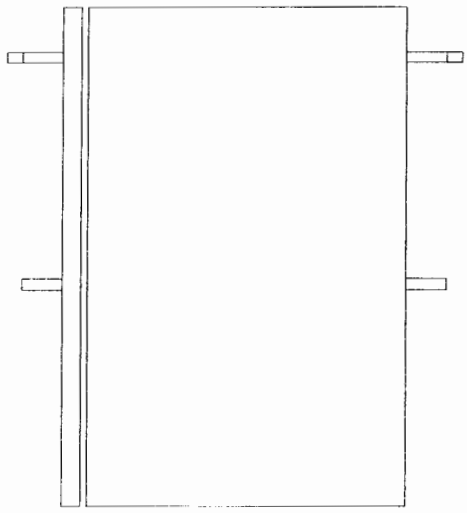

WALL C

Crack patterns at the end of run 4

UNIVERSITY OF PAVIA - EXPERIMENTAL RESULTS

Date 20/06/1994 - Run 5 - Max. nominal drift: 0.20% - WALL B (Window wall)

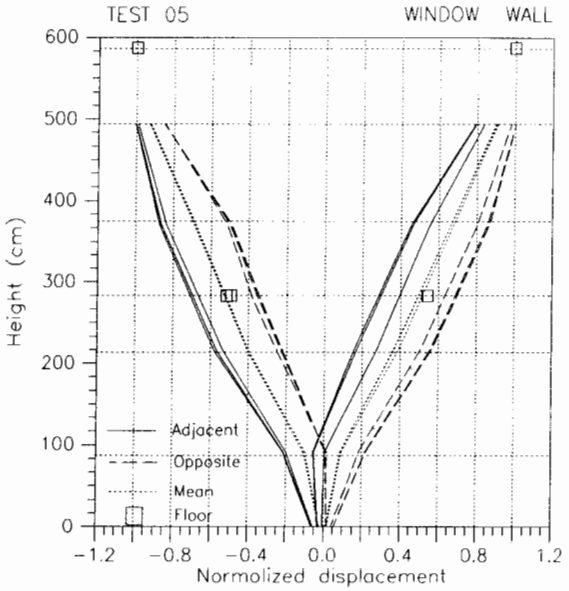

Displaced shape normalized to top floor displacement

Peak	+5'	-5'	+5''	-5''	+5'''	-5'''
Effective drift %	.197	-.198	.199	-.198	.197	-.200
Δ_{h2} (mm)	11.39	-11.45	11.50	-11.46	11.39	-11.53
Δ_{h1} (mm)	6.14	-5.92	6.20	-5.63	6.25	-5.62
Δ_{v2} (mm)	.54	1.38	.68	1.18	.072	1.19
Δ_{v1} (mm)	1.16	.42	1.24	.38	1.12	.44
F_{tot} (kN)	133.5	-128.8	128.9	-108.7	120.9	-106.2
F_2 (kN)	68.9	-65.2	66.7	-55.9	61.8	-54.2
F_1 (kN)	64.6	-63.5	62.2	-52.8	59.1	-52.0

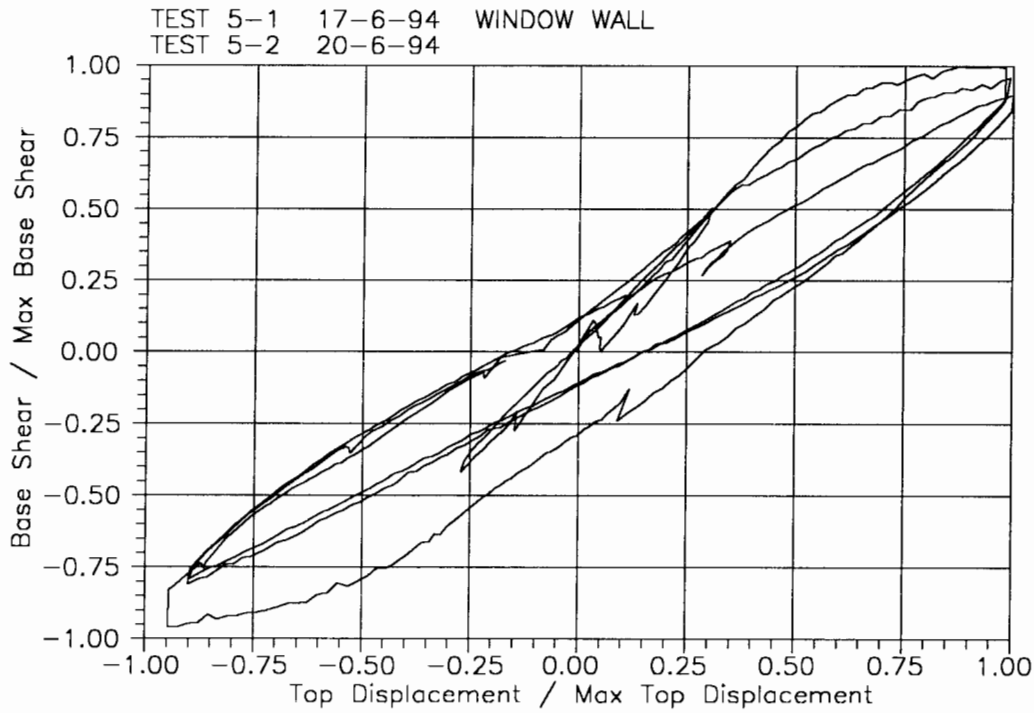

UNIVERSITY OF PAVIA - EXPERIMENTAL RESULTS

Date 20/06/1994 - Run 5 - Max. nominal drift: 0.20% - WALL D (Door wall)

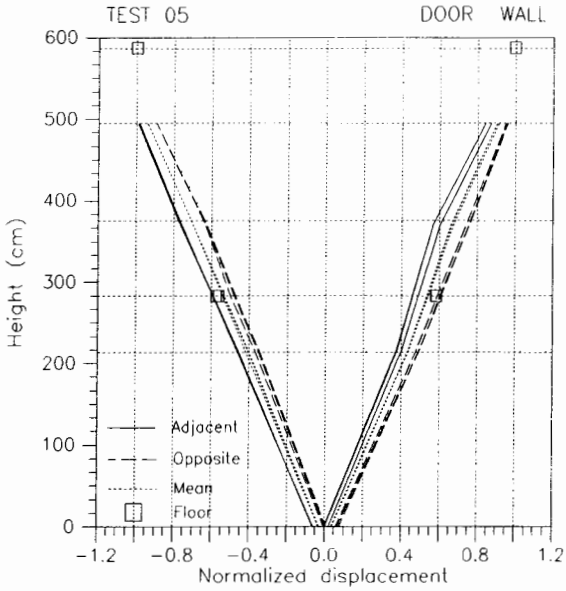

Displaced shape normalized to top floor displacement

Peak	+5'	-5'	+5''	-5''	+5'''	-5'''
Effective drift %	.198	-.199	.199	-.199	.197	-.200
Δ_{h2} (mm)	11.41	-11.47	11.48	-11.46	11.39	-11.53
Δ_{h1} (mm)	6.60	-6.58	6.63	-6.45	6.59	-6.45
Δ_{v2} (mm)	-.41	2.83	-.07	2.51	-.09	2.47
Δ_{v1} (mm)	3.10	-.56	3.10	-.69	2.88	-.71
F_{tot} (kN)	149.4	-135.4	144.7	-126.4	139.8	-124.9
F_2 (kN)	73.6	-73.9	72.3	-63.4	70.5	-63.3
F_1 (kN)	75.8	-61.5	72.4	-63.0	69.3	-61.6

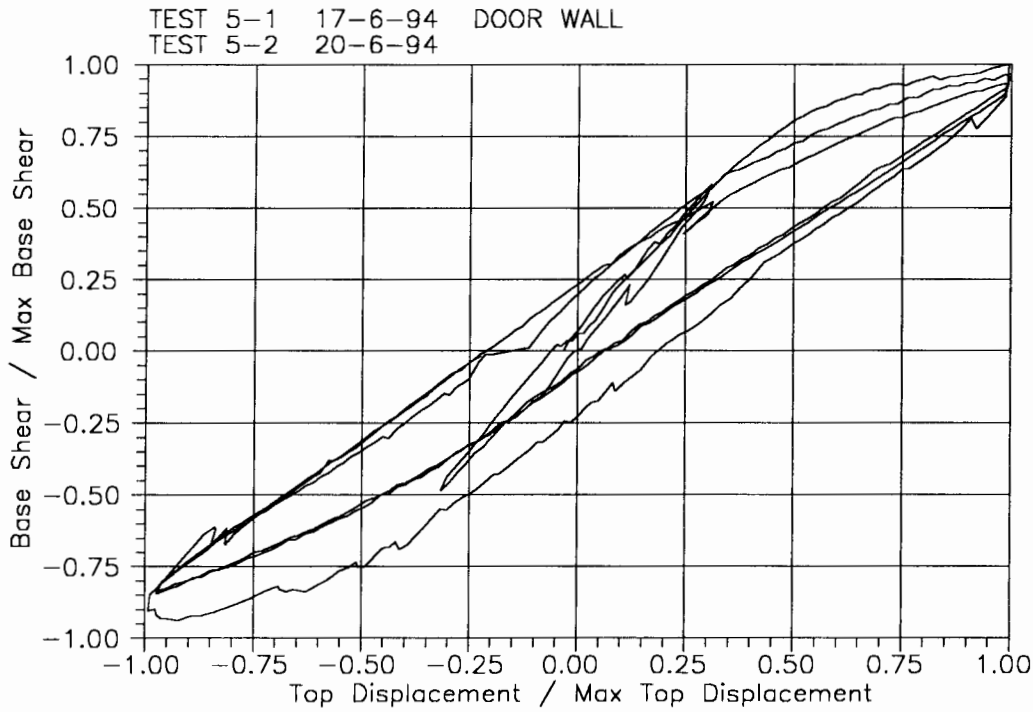

UNIVERSITY OF PAVIA - EXPERIMENTAL RESULTS

Date 20/06/1994 - Run 5 - Max. nominal drift: 0.20%

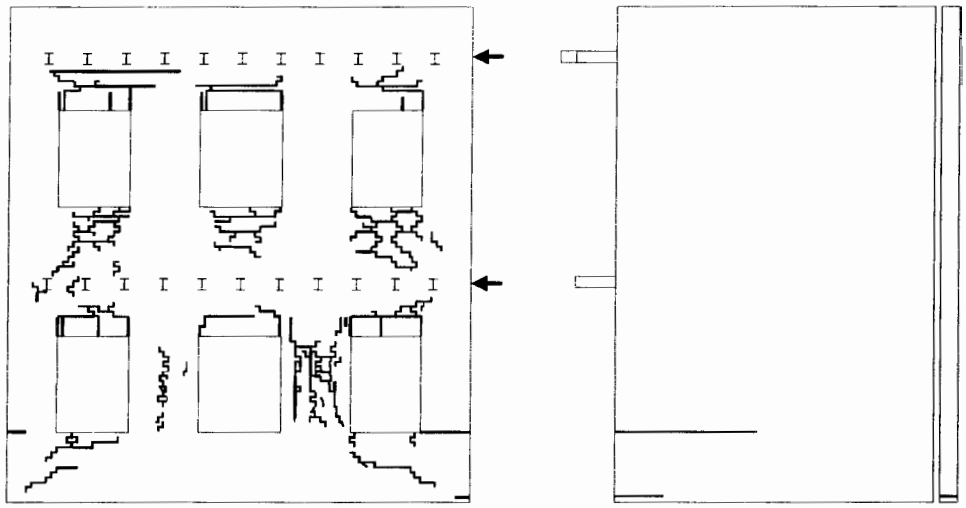

WALL B WALL A

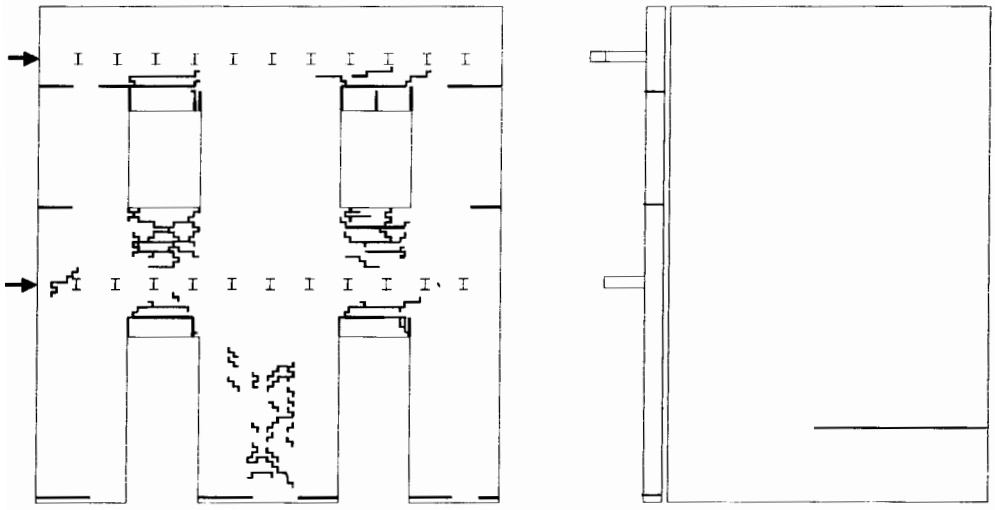

WALL D WALL C

Crack patterns at the end of run 5

UNIVERSITY OF PAVIA - EXPERIMENTAL RESULTS

Date 01/07/1994 - Run 6 - Max. nominal drift: 0.30% - WALL B (Window wall)

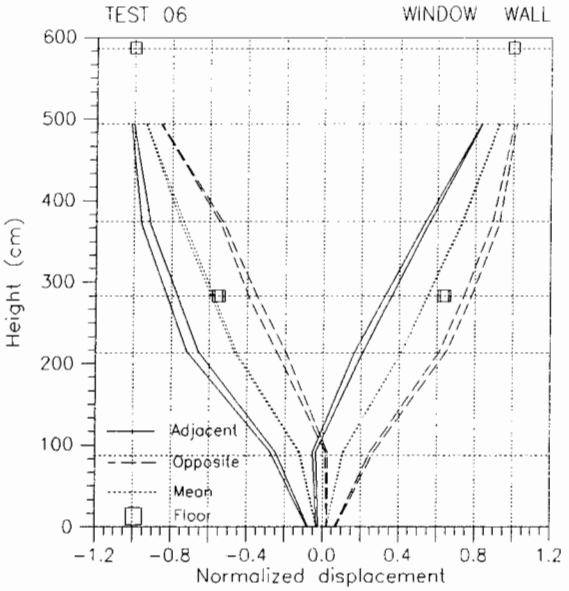

Displaced shape normalized to top floor displacement

Peak	+6'	-6'	+6''	-6''	+6'''	-6'''
Effective drift %	.298	-.298	.299	-.299	.298	-.367
Δ_{h2} (mm)	17.18	-17.17	17.26	-17.24	17.20	-21.19
Δ_{h1} (mm)	10.66	-9.52	10.96	-9.84	10.64	-13.13
Δ_{v2} (mm)	1.01	1.91	1.03	1.56	1.08	1.87
Δ_{v1} (mm)	1.62	.75	1.42	.79	1.25	1.07
F_{tot} (kN)	125.3	-125.9	115.4	-114.1	107.9	-112.4
F_2 (kN)	62.4	-62.5	58.0	-55.6	54.4	-57.5
F_1 (kN)	62.9	-63.4	57.4	-58.5	53.5	-54.9

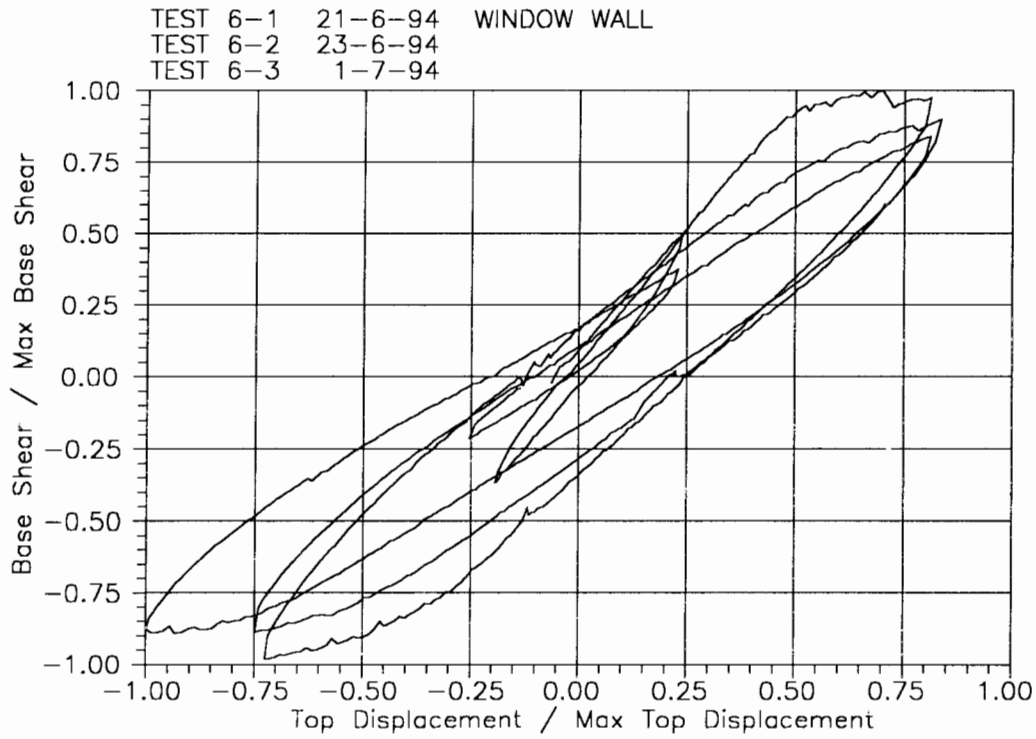

UNIVERSITY OF PAVIA - EXPERIMENTAL RESULTS

Date 01/07/1994 - Run 6 - Max. nominal drift: 0.30% - WALL D (Door wall)

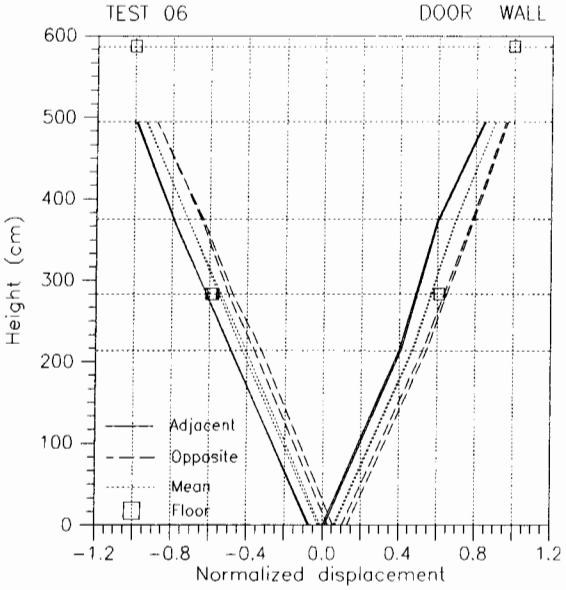

Displaced shape normalized to top floor displacement

Peak	+6'	-6'	+6''	-6''	+6'''	-6'''
Effective drift %	.298	-.298	.299	-.299	.298	-.367
Δ_{h2} (mm)	17.18	-17.17	17.25	-17.24	17.20	-21.19
Δ_{h1} (mm)	10.50	-10.15	10.54	-10.01	10.51	-13.02
Δ_{v2} (mm)	-.05	4.22	-.08	4.09	-.10	4.83
Δ_{v1} (mm)	4.58	-.68	4.33	-.75	3.93	-.70
F_{tot} (kN)	149.7	-141.4	142.2	-138.2	138.3	-137.9
F_2 (kN)	74.7	-70.9	71.9	-68.7	69.9	-71.6
F_1 (kN)	75.0	-70.5	70.3	-69.5	68.4	-66.3

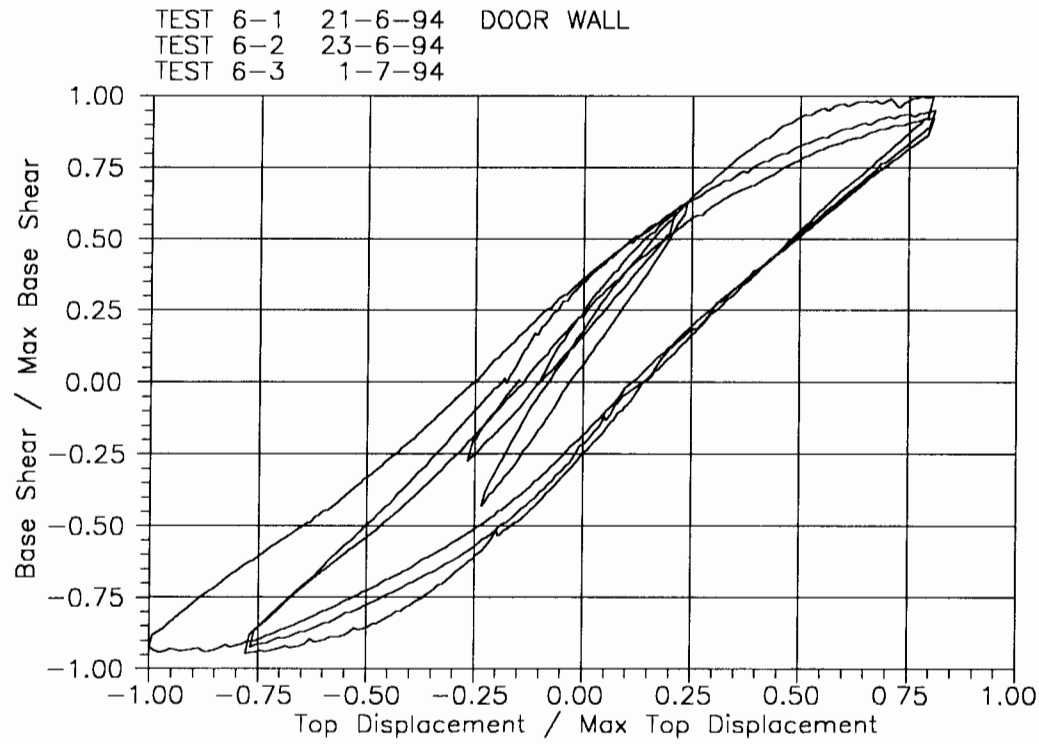

UNIVERSITY OF PAVIA - EXPERIMENTAL RESULTS

Date 01/07/1994 - Run 6 - Max. nominal drift: 0.30%

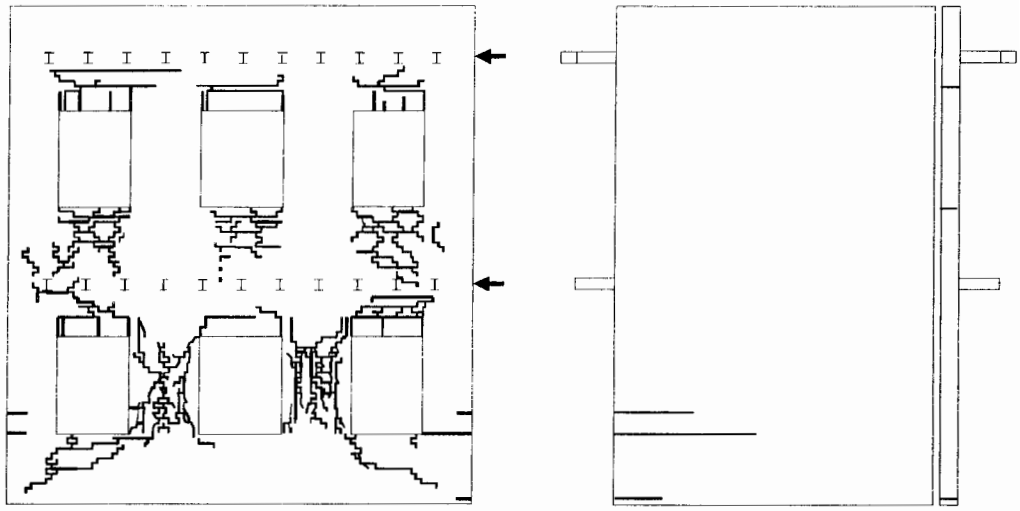

WALL B WALL A

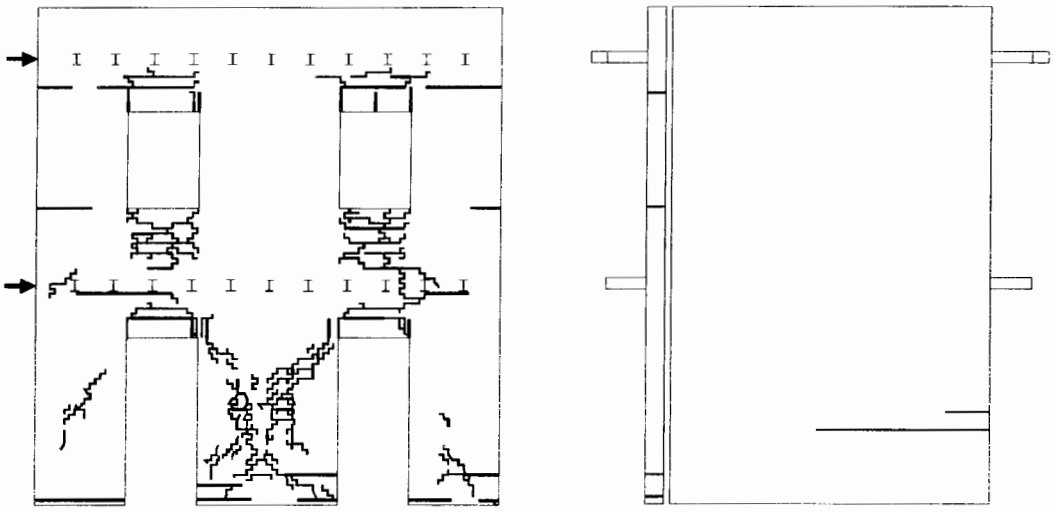

WALL D WALL C

Crack patterns at the end of run 6

UNIVERSITY OF PAVIA - EXPERIMENTAL RESULTS

Date 07/07/1994 - Run 7 - Max. nominal drift: 0.40% - WALL B (Window wall)

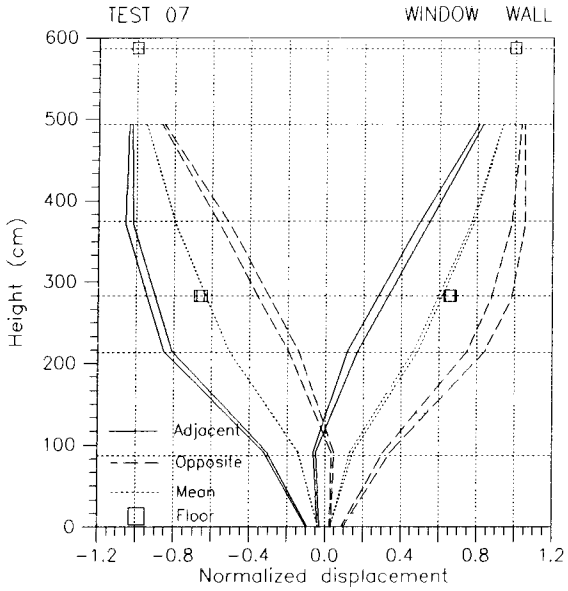

Displaced shape normalized to top floor displacement

Peak	+7'	-7'	+7''	-7''		
Effective drift %	.397	-.432	.379	-.380		
Δ_{h2} (mm)	22.93	-24.94	21.84	-21.90		
Δ_{h1} (mm)	15.16	-16.98	14.00	-14.63		
Δ_{v2} (mm)	1.67	2.25	1.85	1.79		
Δ_{v1} (mm)	1.91	1.49	1.62	1.29		
F_{tot} (kN)	113.3	-109.6	101.3	-91.7		
F_2 (kN)	57.9	-55.4	51.0	-50.3		
F_1 (kN)	55.4	-54.2	50.3	-41.4		

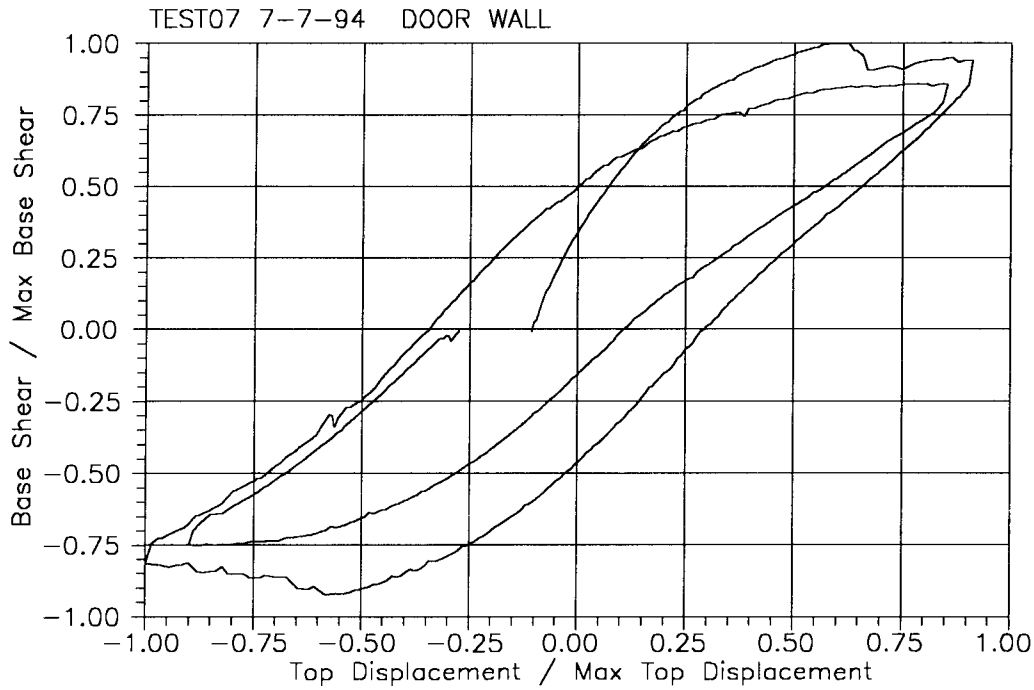

UNIVERSITY OF PAVIA - EXPERIMENTAL RESULTS

Date 07/07/1994 - Run 7 - Max. nominal drift: 0.40% - WALL D (Door wall)

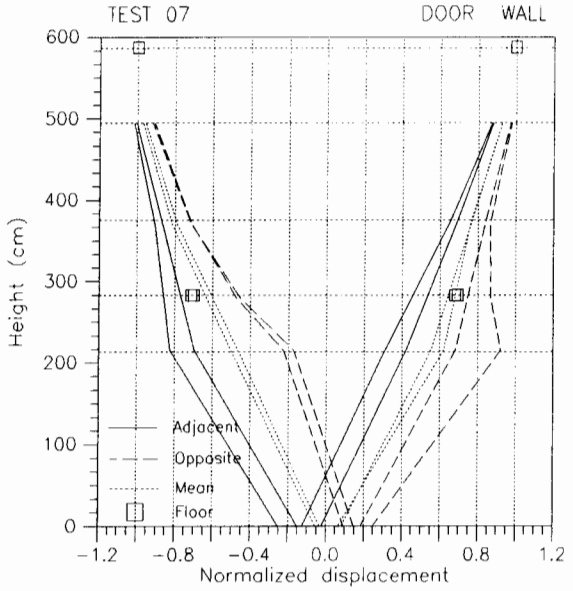

Displaced shape normalized to top floor displacement

Peak	+7'	-7'	+7''	-7''		
Effective drift %	.397	-.432	.379	-.380		
Δ_{h2} (mm)	22.93	-24.94	21.84	-21.90		
Δ_{h1} (mm)	15.89	-17.42	14.85	-15.66		
Δ_{v2} (mm)	0.11	4.76	.83	.359		
Δ_{v1} (mm)	4.37	-.74	4.55	-.42		
F_{tot} (kN)	127.9	-110.8	116.6	-101.6		
F_2 (kN)	62.1	-53.0	62.2	-52.1		
F_1 (kN)	65.8	-57.8	54.4	-49.5		

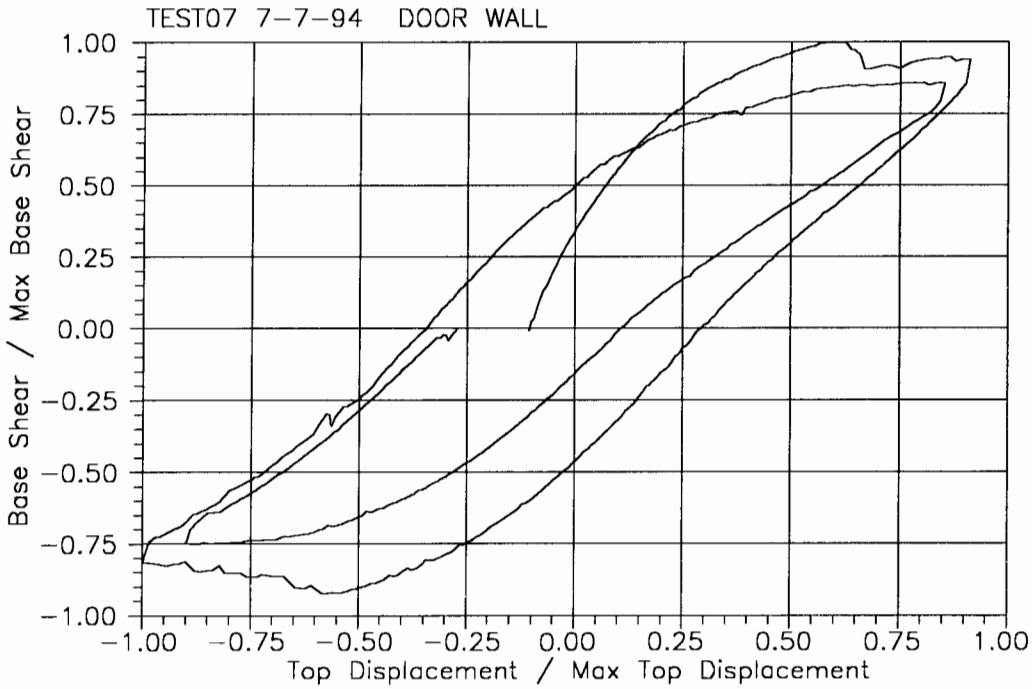

UNIVERSITY OF PAVIA - EXPERIMENTAL RESULTS

Date 07/07/1994 - Run 7 - Max. nominal drift: 0.40%

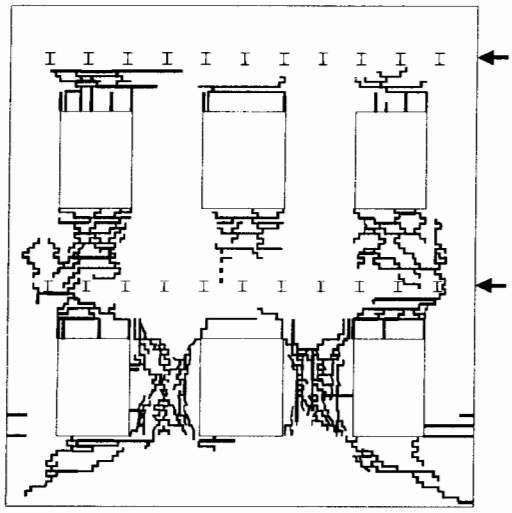

WALL B

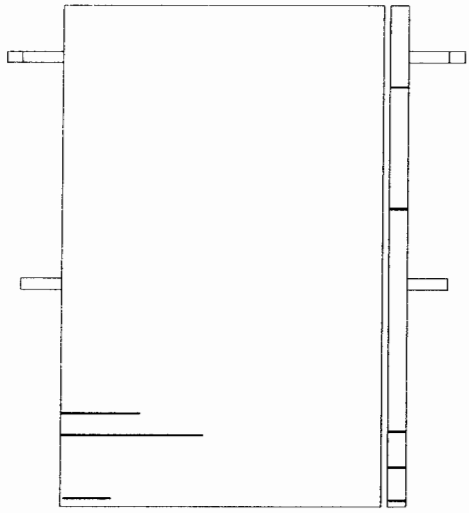

WALL A

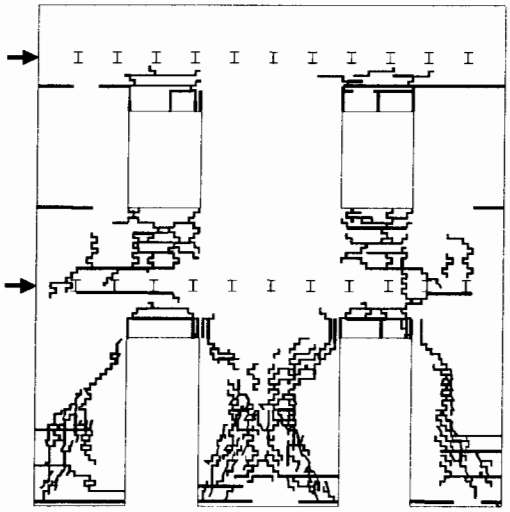

WALL D

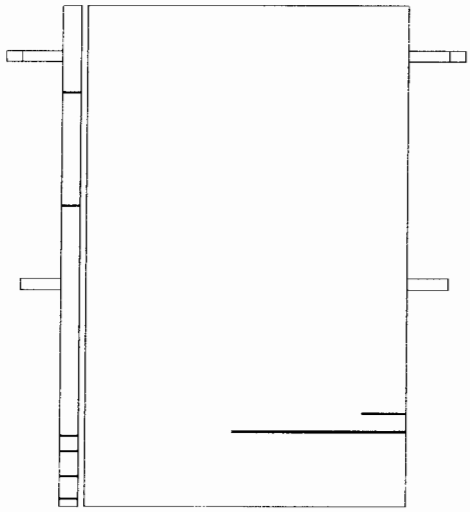

WALL C

Crack patterns at the end of run 7